Oxidation-triggered c-Jun N-terminal kinase (JNK) and p38 mitogen-activated protein (MAP) kinase pathways for apoptosis in human leukaemic cells stimulated by epigallocatechin-3-gallate (EGCG): a distinct pathway from those of chemically induced and receptor-mediated apoptosis

Koichi SAEKI*, Norihiko KOBAYASHI*, Yuko INAZAWA*, Hong ZHANG*, Hideki NISHITOH†, Hidenori ICHIJO†, Kumiko SAEKI*, Mamoru ISEMURA‡ and Akira YUO*[1]

*Department of Haematology, Research Institute, International Medical Centre of Japan, 1-21-1, Toyama, Shinjuku-ku, Tokyo 162-8655, Japan, †Laboratory of Cell Signalling, Graduate School, Tokyo Medical and Dental University, Tokyo 113-8549, Japan, and ‡School of Food and Nutritional Sciences, University of Shizuoka, Shizuoka 422-8526, Japan

We investigated intracellular signalling pathways for apoptosis induced by epigallocatechin-3-gallate (EGCG) as compared with those induced by a toxic chemical substance (etoposide, VP16) or the death receptor ligand [tumour necrosis factor (TNF)]. EGCG as well as VP16 and TNF induced activation of two apoptosis-regulating mitogen-activated protein (MAP) kinases, namely c-Jun N-terminal kinase (JNK) and p38 MAP kinase, in both human leukaemic U937 and OCI-AML1a cells. In U937 cells, the apoptosis and activation of caspases-3 and -9 induced by EGCG but not VP16 and TNF were inhibited with SB203580, a specific inhibitor of p38, while those induced by EGCG and VP16 but not TNF were inhibited with SB202190, a rather broad inhibitor of JNK and p38. In contrast, the EGCG-induced apoptosis in OCI-AML1a cells was resistant to SB203580 but not to SB202190. Unlike TNF, EGCG did not induce the activation of nuclear factor-κB but rather induced the primary activation of caspase-9. *N*-Acetyl-L-cysteine (NAC) almost completely abolished apoptosis induced by EGCG under conditions in which the apoptosis induced by VP16 or TNF was not affected. The JNK/p38 activation by EGCG was also potently inhibited by NAC, whereas those by VP16 and TNF were either not or only minimally affected by NAC. In addition, dithiothreitol also suppressed both apoptosis and JNK/p38 activation by EGCG, and EGCG-induced activation of MAP kinase kinase (MKK) 3/6, MKK4 and apoptosis-regulating kinase 1 (ASK1) was suppressed by NAC. Dominant negative ASK1, MKK6, MKK4 and JNK1 potently inhibited EGCG-induced cell death. EGCG induced an intracellular increase in reactive oxygen species and GSSG, both of which were also inhibited by NAC, and the decreased synthesis of glutathione rendered the cell susceptible to EGCG-induced apoptosis. Taken together these results strongly suggest that EGCG executed apoptotic cell death via an ASK1, MKK and JNK/p38 cascade which is triggered by NAC-sensitive intracellular oxidative events in a manner distinct from chemically induced or receptor-mediated apoptosis.

Key words: apoptosis-regulating kinase 1, caspase, polyphenol, reactive oxygen species, reduction–oxidation.

INTRODUCTION

Green tea and its constituent polyphenols have been shown to possess anti-tumour properties in a wide variety of experimental systems, and epigallocatechin-3-gallate (EGCG) is the most abundant compound among the polyphenols in green tea [1–3]. Several other catechins, such as epigallocatechin (EGC), epicatechin gallate (ECG) and epicatechin (EC), are also known as green tea polyphenols, although the effect of EGCG is the most potent among these catechin compounds [4–6]. The anti-tumour effects of these green tea polyphenols (particularly of EGCG) have recently been studied at the cell biological level, and the major cellular phenomena induced by the catechins were found to be apoptosis and cell cycle arrest [3,6].

Intracellular signalling pathways for apoptosis have mainly focused on two cascades, namely the kinase cascade [7,8] and the protease cascade [8–10]. The former signalling cascade was originally identified as an important pathway in the transduction of apoptotic signals initiated by stress or toxic stimuli, and the major participants in this kinase cascade are two members of the mitogen-activated protein (MAP) kinases, c-Jun N-terminal kinase (JNK) and p38 MAP kinase, as well as their upstream kinases such as MAP kinase kinases (MKKs) [7]. The latter caspase cascade has been thought to play a central role in death receptor-mediated signalling pathways that transduce apoptotic signals from the initiator caspases such as caspase-8 to caspase-activated DNase (CAD) via the executioner caspases such as caspase-3 [9–11]. Identification of CAD which is responsible for internucleosomal DNA fragmentation and its proteolytic activation by caspase-3 shed new light on the molecular basis for the mechanisms of apoptosis [10,11], and the caspase pathways have been intensively studied over recent years [8–11]. However, recent studies by several independent groups have demonstrated the essential role of the kinase cascade as well as its downstream mitochondrial pathway during apoptosis induction by cellular stress, such as UV radiation [12–15].

Abbreviations used: ASK1, apoptosis signal-regulating kinase 1; BSO, buthionine sulphoxide; CAD, caspase-activated DNase; DCFH-DA, 2′,7′-dichlorofluorescin diacetate; DTT, dithiothreitol; EC, epicatechin; ECG, epicatechin gallate; EGC, epigallocatechin; EGCG, epigallocatechin-3-gallate; FBS, fetal bovine serum; GFP, green fluorescent protein; IκB, inhibitory κB; JNK, c-Jun N-terminal kinase; MAP, mitogen-activated protein; MCA, 4-methylcoumaryl-7-amide; MKK, mitogen-activated protein kinase kinase; NAC, *N*-acetyl-L-cysteine; NF-κB, nuclear factor-κB; PI, propidium iodide; ROS, reactive oxygen species; TNF, tumour necrosis factor.

[1] To whom correspondence should be addressed (e-mail yuoakira@ri.imcj.go.jp).

Mechanisms by which catechin compounds such as EGCG induce apoptotic cell death are still largely unknown. A recent study showed the involvement of caspase-3 during apoptosis of chondrosarcoma cells stimulated by EGCG [16], although the pathway from catechin to caspase-3 is not clear. It is possible that polyphenols might utilize the kinase cascade in a similar manner to toxic substances or cellular stress. Alternatively, catechins, which are water-soluble substances with limited ability to pass through the plasma membrane of cells may bind to certain cell surface receptors, thereby provoking death receptor-like intracellular signals.

In the present study, we investigated the effects of EGCG on the intracellular apoptotic signal transduction system in human leukaemic cells, mainly focusing on the MAP kinase cascade, and compared this with the pathways for the two typical types of apoptosis induced by established stimuli [17]. In this study, etoposide (VP16) and tumour necrosis factor (TNF) were used as the representatives of a chemical (toxic) substance and death-receptor agonist, respectively. U937 cells were used as the main targets since this cell line responded to EGCG with apoptotic cell death but not with cell cycle arrest (as shown in this study). Our results strongly suggest an essential role for the JNK and/or p38 pathway(s) during the execution of apoptosis and caspase activation by EGCG. In addition, we found that certain targets of *N*-acetyl-L-cysteine (NAC) and dithiothreitol (DTT), such as intracellular oxidation and/or reactive oxygen species (ROS), were located proximal to the MAP kinase cascade in the EGCG signalling pathway, and that apoptosis-regulating kinase 1 (ASK1), which might be controlled by the redox balance, seems to play a significant role in the upstream mechanism. Several interesting differences between EGCG-induced apoptosis and chemically induced or receptor-mediated apoptosis are also presented and discussed.

EXPERIMENTAL

Materials

All catechin derivatives, EGCG, EGC, ECG, EC and (+)-catechin, were purchased from Funakoshi Co., Tokyo, Japan. These catechin derivatives used in this study were > 98 % pure. Highly purified (> 98 %) recombinant human TNF produced by *Escherichia coli* was purchased form PeproTech EC, London, U.K., and highly purified (> 98 %) recombinant human granulocyte colony-stimulating factor produced by *E. coli* was kindly provided by Kirin Brewery Co., Tokyo, Japan. Propidium iodide (PI), buthionine sulphoxide (BSO), NAC and VP16 were purchased from Sigma, St. Louis, MO, U.S.A.; annexin V–phycoerythrin was from BioVision, Mountain View, CA, U.S.A.; proteinase K was from Boehringer Mannheim, Mannheim, Germany; DTT, RNase and urokinase were from Wako Pure Chemical Co., Tokyo, Japan; SYBR Green I was from Molecular Probes, Eugene, OR, U.S.A.; Hi-Lo™ DNA Marker was from Abetech, Tokyo, Japan; poly(dI-dC) was from Boehringer Mannheim; fluorogenic substrate for urokinase (Glt-Gly-Arg-MCA; where MCA is 4-methylcoumaryl-7-amide) was from Peptide Institute, Osaka, Japan; 2′,7′-dichlorofluorescin diacetate (DCFH-DA) was from Molecular Probes; ApoAlert® Glutathione Detection Kit was from Clontech Laboratories, Palo Alto, CA, U.S.A.; and Bioxytech® GSH/GSSG-412™ was from OXIS Health Products, Portland, OR, U.S.A.

Polyclonal anti-phosphorylated ASK1 antibody was produced by immunizing rabbits with a synthetic phospho-Thr^{845} peptide (CTET*FTGTLQY; where T* is phosphorylated threonine) corresponding to residues around Thr^{845} of human ASK1 [18]. The polyclonal antibodies against JNK, p38, Thr^{183}/Tyr^{185}-phosphorylated JNK, Thr^{180}/Tyr^{182}-phosphorylated p38, Thr^{223}-phosphorylated MKK4 and Ser$^{189/207}$-phosphorylated MKK3/MKK6 were from New England Biolabs, Beverly, MA, U.S.A.; polyclonal anti-MKK3 and anti-MKK4 was from Upstate Biotechnology, Lake Placid, NY, U.S.A.; anti-β-tubulin antibody was from Santa Cruz Biotechnology, Santa Cruz, CA, U.S.A.; monoclonal anti-caspase-3 antibody was from BD Transduction Laboratories, Lexington, KY, U.S.A.; monoclonal anti-caspase-9 and anti-caspase-8 antibodies were from Medical & Biological Laboratories Co., Nagoya, Japan; polyclonal anti-cleaved-caspase-9 antibody D315 (which specifically recognizes the Apaf-1 autoactivation site at Asp-315) and polyclonal anti-inhibitory κB (IκB)-α antibody were from Cell Signalling Technology, Beverly, MA, U.S.A.; horseradish peroxidase-conjugated anti-rabbit and anti-mouse antibodies were from Cell Signalling Technology; horseradish peroxidase-conjugated anti-sheep IgG antibody was from Upstate Biotechnology; and SuperSignal West Femto Maximum Sensitivity Substrate was from Pierce, Rockford, IL, U.S.A.

SDS was purchased from Wako Pure Chemical Co; SB203580 and SB202190 were from Calbiochem-Novabiochem Co., La Jolla, CA, U.S.A.; PVDF membrane was from Millipore Japan Co., Tokyo, Japan; skimmed milk was from Snow Brand Industry, Tokyo, Japan; RPMI 1640 medium was from Gibco Laboratories, Grand Island, NY, U.S.A.; and fetal bovine serum (FBS) was from JRH Bioscience, Lenexa, KS, U.S.A. SP600125, a highly specific inhibitor of JNK [19], was kindly provided by Dr Brydon L. Bennett (Celgene Corporation, San Diego, CA, U.S.A.). Expression vectors for dominant negative ASK1, MKK6, MKK4, MKK7 and JNK1 [pcDNA3-HA-ASK1-KM, pME-HA-MKK6AA, pGFP-SEK1K-R, pcDLSRα-Myc-MKK7KL and pCR3JNK1β1(APF)] were described previously [20–23]. Dominant negative MKK7 was kindly provided by Professor Eisuke Nishida (Kyoto University, Kyoto, Japan). Dominant negative MKK6 and JNK1 were kindly provided by Professor Fuyuki Ishikawa (Kyoto University) and Dr Chifumi Kitanaka (National Cancer Centre, Tokyo, Japan) under the permission of Professor Eisuke Nishida and Dr Hiroyuki Seimiya (Japanese Foundation for Cancer Research, Tokyo, Japan), respectively. pEGFP-C1 and pCI-neo were purchased from Clontech Laboratories and Promega, Madison, WI, U.S.A., respectively. All other reagents in the present experiments were purchased from Sigma.

Culture and preparation of cells

Human leukaemic U937 cells were grown in RPMI 1640 medium supplemented with 10 % heat-inactivated FBS, penicillin (100 units/ml) and streptomycin (100 μg/ml). Human leukaemic OCI-AML1a cells [24] were kindly provided by Professor Nobuo Nara at the Tokyo Medical and Dental University, Tokyo, Japan, and were grown in RPMI 1640 medium supplemented with 10 % heat-inactivated FBS, penicillin (100 units/ml) and streptomycin (100 μg/ml) in the presence of 10 ng/ml granulocyte colony-stimulating factor. For the induction of apoptosis, U937 and OCI-AML1a cells were seeded at 1×10^6 cells/ml and grown in the presence or absence of the relevant agents for up to 6 h. After the incubation, the cells were harvested and washed three times with PBS, before being suspended in the appropriate buffer for each experiment.

Western blotting

U937 cells and OCI-AML1a cells suspended in RPMI 1640 medium with 10 % FBS were prewarmed for 10 min at 37 °C, and then treated with inhibitors and/or stimulated with a

cytotoxic agent or cytokine for the indicated periods at 37 °C. The reactions were terminated by rapid centrifugation, and the pellets frozen in liquid nitrogen after aspiration of the supernatant. The cell pellets were resuspended in an ice-cold solution containing 50 mM Hepes, pH 7.4, 1 % Triton X-100, 2 mM sodium orthovanadate, 100 mM NaF, 1 mM EDTA, 1 mM EGTA, 1 mM PMSF, 10 μg/ml aprotinin and 10 μg/ml leupeptin. The cell suspensions were then mixed 1:1 with 2 × sample buffer (4 % SDS, 20 % glycerol, 10 % mercaptoethanol and a trace amount of Bromphenol Blue dye in 125 mM Tris/HCl, pH 6.8) and heated to 100 °C for 5 min. These denatured samples were loaded on to an SDS/polyacrylamide gel, and after electrophoresis the proteins were electrotransferred on to a PVDF membrane in a buffer (25 mM Tris, 192 mM glycine and 20 % methanol) with 2 mA/cm² for 2 h at 4 °C. Residual binding sites on the membrane were blocked by incubation in PBS with 0.05 % Tween 20 and 5 % skimmed milk. The membranes were then incubated with the primary antibody in PBS with 0.05 % Tween 20 and 1 % skimmed milk for 4 h at 25 °C. The primary antibody was removed and the blots washed three times in PBS with 0.05 % Tween 20. To detect the antibody reactions, the blots were incubated for 2 h with horseradish peroxidase-conjugated anti-mouse, anti-rabbit or anti-sheep IgG antibody diluted 1:200000 in PBS with 0.05 % Tween 20 and 1 % skimmed milk, before being washed intensively in PBS with 0.05 % Tween 20, and then placed in a SuperSignal West Femto Substrate working solution for 5 min at 25 °C. The blots were then removed from the working solution, and exposed to the film.

Determination of DNA fragmentation

The detection of internucleosomal DNA fragmentation was performed as described by Sellins and Cohen [25] with some modifications. For this, 4×10^5 cells were suspended in 100 μl of hypotonic lysis buffer (0.2 % Triton X-100, 1 mM EDTA and 10 mM Tris/HCl, pH 7.5), and incubated for 20 min at 4 °C. After centrifugation for 5 min at 14000 ***g***, the supernatant was collected and incubated with RNase A (final concentration, 200 μg/ml) for 1 h at 37 °C followed by a digestion with proteinase K (final concentration, 200 μg/ml) for 30 min at 50 °C. The fragmented DNA was then precipitated overnight at −20 °C in 50 % isopropanol and 0.5 M NaCl. The precipitates were pelleted by centrifugation for 10 min at 14000 ***g***, air-dried and resuspended in buffer containing 1 mM EDTA and 10 mM Tris/HCl, pH 7.4. Loading buffer containing 15 mM EDTA, 2 % SDS, 50 % glycerol and 0.5 % Bromophenol Blue was added to the samples at a 1:5 (v/v) ratio, and the samples heated to 65 °C for 10 min. Horizontal electrophoresis of the samples and molecular marker(s) was performed with a 2 % agarose gel and 0.5 × TBE buffer (Tris/borate/EDTA buffer; 45 mM Tris/borate and 1 mM EDTA) at 90 V, using a MUPID-2 mini electrophoretic system (Cosmo Bio Co., Tokyo, Japan). After electrophoresis, the gels were stained with SYBR Green I and the fragmented DNA imaged using a FluorImager (Amersham Biosciences, Tokyo, Japan).

Flow cytometry analysis for the determination of apoptosis

Cell cycle analysis for the determination of the sub-G_1 region was performed as described [26]. Cells were washed in PBS and resuspended in 70 % ice-cold ethanol for fixing. After treatment with RNase (100 μg/ml) for 30 min at 37 °C, DNA was stained with 50 μg/ml PI for 30 min on ice. Determination of cell cycle distribution was performed by FACS Calibur (Nippon Becton Dickinson Co., Tokyo, Japan) and the number of cells in the area corresponding to the sub-G_1 region was calculated using Cell Quest (Nippon Becton Dickinson Co.). For the determination of annexin V positivity, cells were washed in PBS and resuspended in staining buffer (PBS containing 5 % FBS and 0.05 % sodium azide). After treatment with annexin V–phycoerythrin for 5 min at room temperature, one-colour analyses were performed using a FACS Calibur.

Transient transfection and cell death assay

Efficient transfection of DNA was performed using Nucleofector technology (Amaxa GmbH, Cologne, Germany) as described in [27]. 2×10^6 cells were suspended in 100 μl of transfection medium (Nucleofector solution V) in the electroporation cuvette. After adding 2 μg of plasmid DNA {1 μg of pEGFP-C1 [green fluorescent protein (GFP) expression vector] and 1 μg of pCI-neo (control) or expression vectors for dominant negative mutants}, electroporation was performed using programmes provided by the manufacturer. Immediately after electroporation, cells were suspended in 1.5 ml of culture medium (RPMI 1640 medium supplemented with 10 % heat-inactivated FBS) in a 12-well multi-well plate, and were then incubated for 4 h at 37 °C. After replacing with new culture medium, cells were incubated for another 20 h at 37 °C. After incubation, cells were stimulated with 400 μM EGCG for 4 h at 37 °C, and were suspended in staining buffer in the presence of 1 μg/ml PI, and two-colour analyses were performed using a FACS Calibur. Only GFP-positive transduced cells were counted for PI positivity, and the quantity of dead cells was expressed as percentage of PI-positive cells in the GFP-positive cells. Transfection efficiency (GFP-positive cells/total cells) was approx. 30–40 % in U937 cells and 60–80 % in OCI-AML1a cells in this experimental system.

Electrophoretic mobility shift assay

Activation of nuclear factor-κB (NF-κB) was evaluated by the electrophoretic mobility shift assay with a double-stranded oligonucleotide containing a κB site from the mouse κ-light chain enhancer (5′-AGCTTCAGAGGGGACTTTCCGAGAGG-3′ and 5′-TCGACCTCTCGGAAAGTCCCCTCTGA-3′) as a probe. The nuclear extracts were prepared as described by Schreiber et al. [28] with the following modifications. Cells were lysed with buffer A (1.5 mM $MgCl_2$, 10 mM KCl, 0.5 mM DTT, 0.2 mM phenylmethylsulphonyl fluoride, 10 mM Hepes-KOH, pH 7.9), for 10 min at 4 °C, and this was followed by vortexing to shear the cytoplasmic membranes. Nuclei were pelleted by centrifugation at 10000 ***g*** for 10 s at 4 °C. Nuclear proteins were extracted with high salt buffer C (420 mM NaCl, 1.5 mM $MgCl_2$, 0.2 mM EDTA, 0.5 mM DTT, 0.2 mM PMSF, 25 % glycerol and 20 mM Hepes/KOH, pH 7.9) for 2 min at 4 °C and stored at −80 °C until use. A 5 μg aliquot of the nuclear extract was incubated with labelled probe for 30 min at 30 °C in binding-reaction buffer (75 mM NaCl, 1.5 mM EDTA, 1.5 mM DTT, 7.5 % glycerol, 0.3 % Nonidet P-40, 1 mg/ml BSA and 15 mM Tris/HCl, pH 7.0) in the presence of 2 μg of poly(dI-dC). The total volume of the reaction was 20 μl. DNA–protein complexes were separated from unbound oligonucleotides on a native 4 % polyacrylamide gel in 0.5 × TBE buffer. The gels were then vacuum dried and subjected to autoradiography.

Determination of urokinase activity

Urokinase (20 units) was preincubated with 400 μM EGCG in the presence or absence of 5 mM NAC, and was then incubated

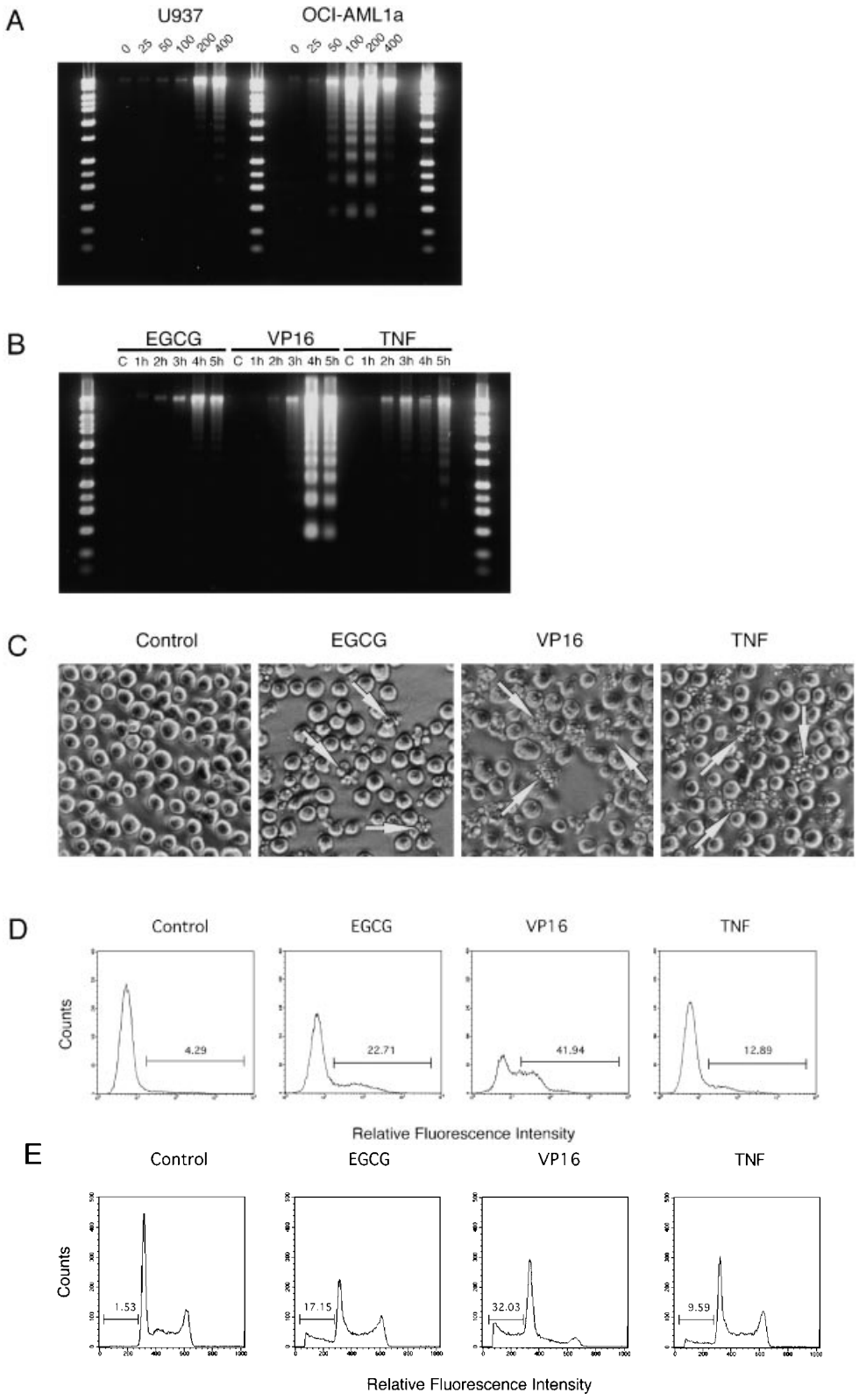

Figure 1 Apoptotic cell death of U937 and OCI-AML1a cells stimulated by EGCG, VP16 and TNF

(**A**) U937 and OCI-AML1a cells were incubated with the indicated concentrations (25–400 μM) of EGCG for 4 h at 37 °C. The presence of internucleosomal DNA fragmentation was examined by agarose gel electrophoresis. (**B**) U937 cells were incubated with the optimal concentrations of EGCG (400 μM), VP16 (10 μg/ml) or TNF (100 ng/ml) for the periods indicated (1–5 h) at 37 °C. The presence of internucleosomal DNA fragmentation was examined by agarose gel electrophoresis. C, control. (**C**) U937 cells were incubated with the optimal concentrations of EGCG, VP16 or

with 5 μM of the fluorescent peptide substrate (Glt-Gly-Arg-MCA) in a reaction buffer (100 mM NaCl, 10 mM $CaCl_2$ and 50 mM Tris/HCl, pH 8.0) for 1 h at 37 °C. After stopping the reaction with 100 mM sodium acetate (pH 4.0), cleavage of the peptide substrate as determined by the release of MCA was measured with a Hitachi F-4010 fluorescence spectrophotometer (Hitachi, Tokyo, Japan). The excitation and emission wavelengths were set at 380 and 460 nm, respectively.

Determination of intracellular ROS

The intracellular concentration of ROS was measured using DCFH-DA as a probe. This probe is a non-polar compound which readily diffuses into cells, where it is hydrolysed to the non-fluorescent polar derivative 2′,7′-dichlorofluorescin and thereby trapped within the cells. In the presence of a proper oxidant, 2′,7′-dichlorofluorescin is oxidized to the highly fluorescent 2′,7′-dichlorofluorescein. After loading of the probe, 4×10^5 cells were incubated with the agonists for the periods indicated at 37 °C, and then placed in a 96-well multi-well plate. The fluorescence of 2′,7′-dichlorofluorescein in the well was visualized using a FluorImager (Amersham Biosciences). The excitation and emission wavelengths were set at 488 and 530 nm, respectively. Fluorescence intensity per well (per 4×10^5 cells) was quantified and calculated using the ImageQuant™ program (Amersham Bioscience).

Determination of intracellular GSH levels

The relative amount of intracellular GSH was measured using an ApoAlert® Glutathione Detection Kit (Clontech Laboratories). Briefly, after solubilization of the cells, the lysate was incubated with 2 mM monochlorobimane for 30 min at 37 °C, and then the fluorescence was measured with a Hitachi F-4010 fluorescence spectrophotometer. The excitation and emission wavelengths were set at 395 and 480 nm, respectively. For the exact determination of total GSH and GSSG (glutathione disulphide) in the presence of NAC, we used another assay kit (Bioxytech® GSH/GSSG-412™). 5,5′-Dithiobis-2-nitrobenzoic acid was used as a chromogen in this assay kit, and 1-methyl-2-vinyl-pyridinium trifluoromethane sulphonate was used as an agent for derivatizing reduced GSH in the determination of GSSG. Absorbance of the reaction mixture in the cuvette was measured at 412 nm using a DU® 530 Life Science UV/Vis Spectrophotometer (Beckman Instruments, Fullerton, CA, U.S.A.).

Statistical analysis

The Student's *t* test was used to determine statistical significance.

RESULTS

Induction of apoptosis in U937 and OCI-AML1a cells stimulated by EGCG

In the initial experiments, we studied the dose- and time-dependency of apoptosis in human leukaemic U937 cells as determined by DNA fragmentation and morphology. As shown in Figure 1(A), EGCG induced DNA fragmentation of U937 cells in a dose-dependent manner and the maximal effect was obtained at 400 μM. EGCG at 400 μM induced DNA fragmentation of U937 cells in a time-dependent manner (Figure 1B). For comparison, chemically induced (or toxic substance-induced) apoptosis and death-receptor-mediated apoptosis were investigated in the same cell line using VP16 and TNF, respectively (Figure 1B). The optimal concentrations of both agents (10 μg/ml for VP16 and 100 ng/ml for TNF) also induced DNA fragmentation of U937 cells with very similar time courses to EGCG, although the effect of TNF was slightly faster. Morphological changes characteristic of apoptotic cell death were observed under the inverted microscope in U937 cells stimulated with 400 μM EGCG, 10 μg/ml VP16 and 100 ng/ml TNF (Figure

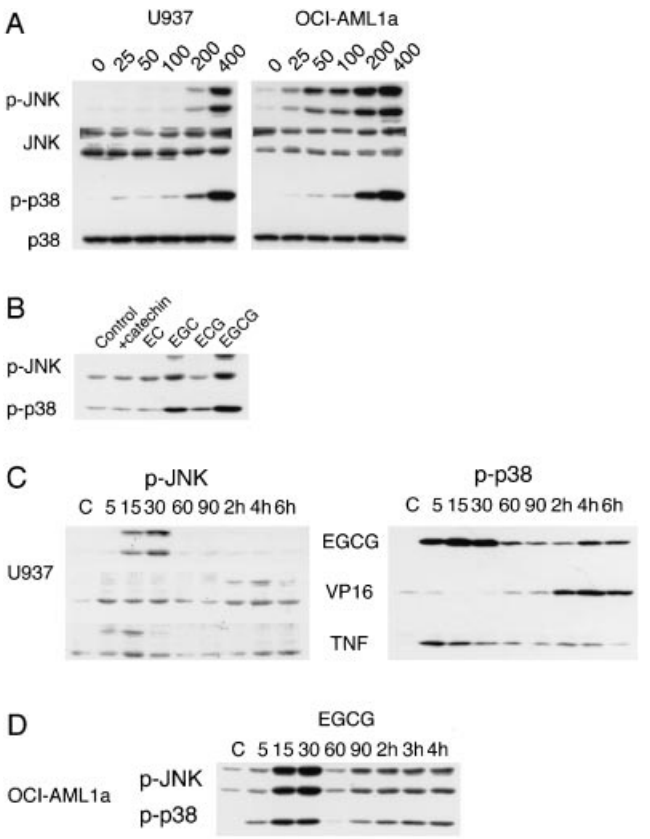

Figure 2 Activation of JNK and p38 in U937 and OCI-AML1a cells stimulated by EGCG, VP16 and TNF

(**A**) U937 (left-hand panel) and OCI-AML1a cells (right-hand panel) were stimulated with the indicated concentrations (25–400 μM) of EGCG for 30 min at 37 °C. Activation states of JNK and p38 were evaluated by Western blotting using antibodies specific for phosphorylated and activated forms of JNK and p38, respectively. (**B**) U937 cells were stimulated with 400 μM of the catechin derivatives (+)-catechin, EC, EGC, ECG and EGCG for 30 min at 37 °C. Activation states of JNK and p38 were evaluated as in (**A**). (**C**) U937 cells were stimulated with the optimal concentrations of EGCG (400 μM), VP16 (10 μg/ml) or TNF (100 ng/ml) for the indicated periods (5 min–6 h) at 37 °C. Activation states of JNK (left-hand panel) and p38 (right-hand panel) were evaluated as in (**A**). (**D**) OCI-AML1a cell were stimulated with the optimal concentrations of EGCG (200 μM) for the indicated periods (5 min–4 h) at 37 °C. Activation states of JNK and p38 were evaluated as in (**A**).

TNF (as above) for 4 h at 37 °C, and were then observed under the inverted microscope. Phase-contrast micrographs are shown and the white arrows represent apoptotic cells. Original magnification, ×200. (**D**) U937 cells were incubated with the optimal concentrations of EGCG, VP16 or TNF (as above) for 4 h at 37 °C, and the positivity for annexin V was determined using FACS Calibur. The percentage of annexin V–phycoerythrin-positive cells is indicated in each panel. (**E**) U937 cells were incubated with the optimal concentrations of EGCG, VP16 or TNF (as above) for 4 h at 37 °C, and were then subjected to cell cycle analysis using FACS Calibur. The percentage of cells in the sub-G_1 region is indicated in each panel.

1C). Roughly estimated, magnitude of apoptosis as determined by morphology was VP16 > EGCG > TNF. To examine the apoptosis on a more quantitative basis, we also determined positivity of cell surface annexin V, and found that EGCG-induced apoptosis was less than VP16-induced apoptosis and more than TNF-induced apoptosis (Figure 1D). According to the cell cycle analysis, substantial increase in the sub-G_1 region was observed in U937 cells stimulated by 400 μM EGCG, 10 μg/ml VP16 and 100 ng/ml TNF (Figure 1E). VP16, but not EGCG and TNF, induced an apparent decrease in S- and G_2/M-phase cells (Figure 1E).

In another human leukaemic cell line OCI-AML1a, EGCG also induced DNA fragmentation in a dose-dependent manner, although lower concentrations of EGCG effectively induced DNA fragmentation in this cell line compared with U937 cells (Figure 1A). Morphological changes characteristic of apoptotic cell death were also observed in this cell line after incubation with EGCG, as based upon the microscopic examination of cultured cells (results not shown).

Activation of JNK and p38 in U937 and OCI-AML1a cells stimulated by EGCG

We then studied the effect of EGCG on JNK and p38, two well-known members of the MAP kinases which are responsible for apoptosis, in U937 and OCI-AML1a cells as determined by immunoblotting using specific antibodies that recognize phosphorylated and activated forms of these two kinases. As shown in Figure 2(A), EGCG induced activation of both JNK and p38 in a dose-dependent manner in both cell lines. The optimal concentration for this effect was 400 μM in U937 cells (Figure 2A, left-hand panel), which is in parallel with the concentrations required for apoptosis of this cell line (Figure 1A). Almost the

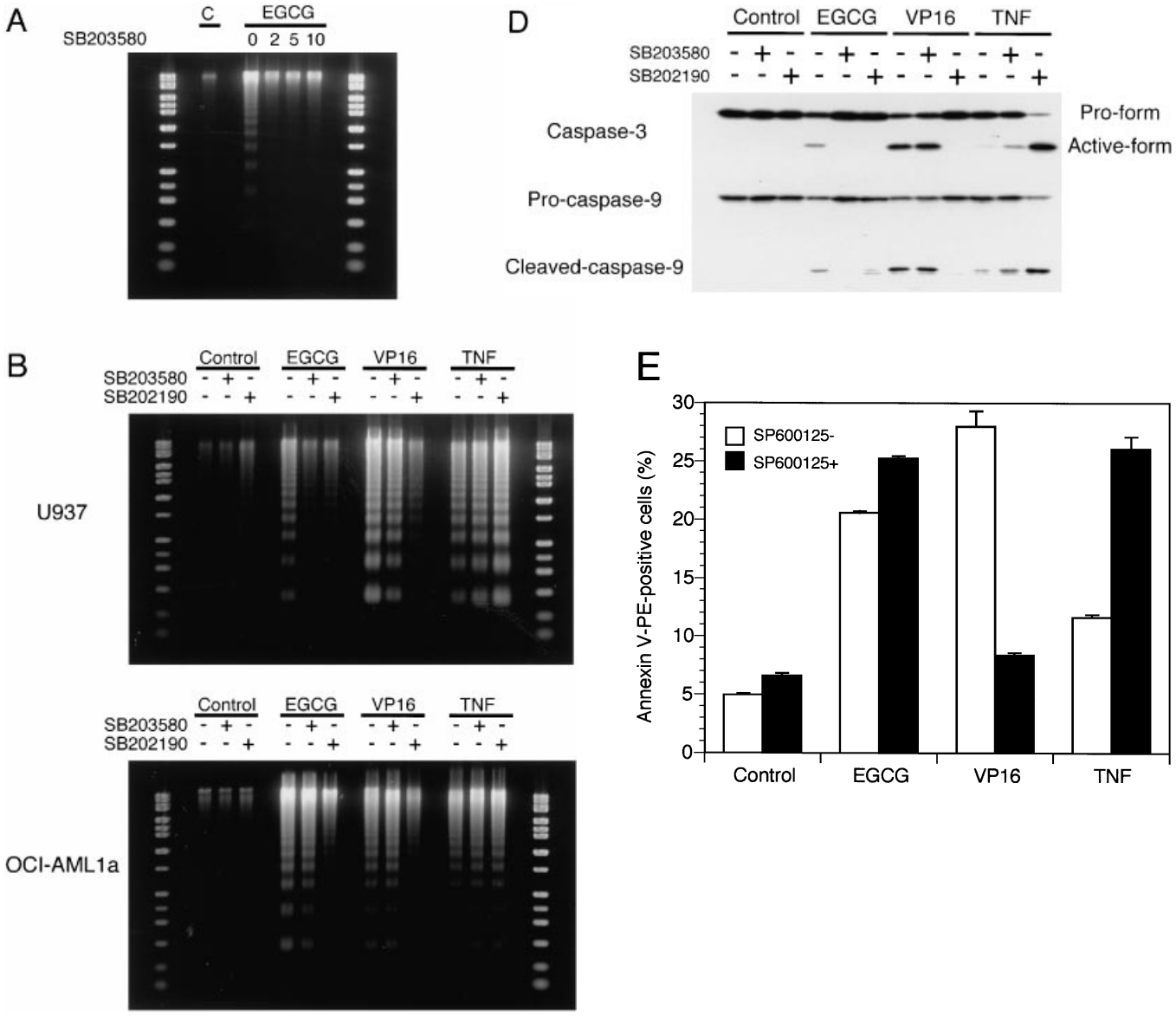

Figure 3 For legend, see facing page.

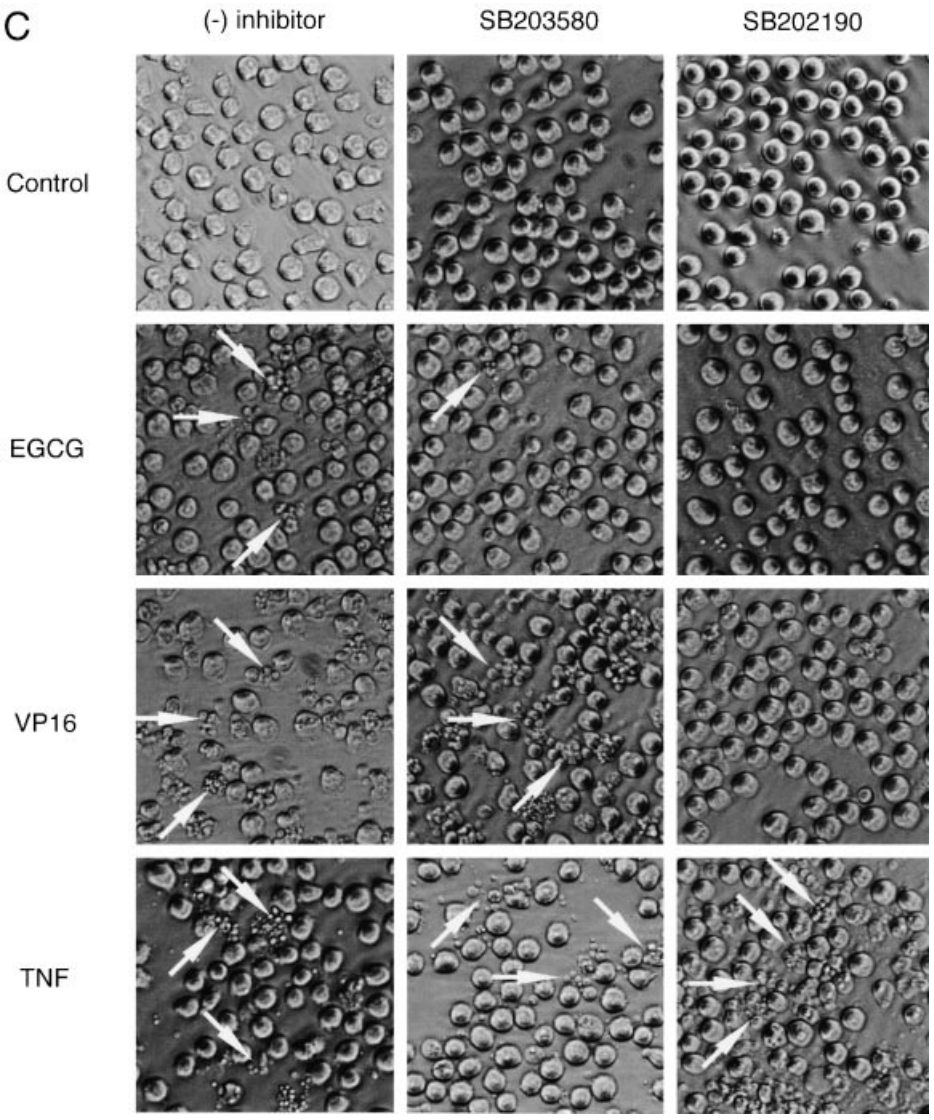

Figure 3 Effects of SB203580 and SB202190 on apoptosis of U937 and OCI-AML1a cells stimulated by EGCG, VP16 and TNF

(**A**) U937 cells were preincubated with the indicated concentrations (2, 5 and 10 μM) of SB203580 for 30 min at 37 °C, and were then stimulated with 400 μM EGCG for 4 h at 37 °C. C, control. (**B**) U937 (upper panel) and OCI-AML1a cells (lower panel) were preincubated with 2 μM SB203580 or 40 μM SB202190 for 30 min at 37 °C, and were then stimulated with the optimal concentrations of EGCG (400 μM for U937 cells and 200 μM for OCI-AML1a cells), VP16 (10 μg/ml) or TNF (100 ng/ml) for 4 h. For (**A**) and (**B**) the presence of internucleosomal DNA fragmentation was examined by agarose gel electrophoresis. (**C**) U937 cells were preincubated with 2 μM SB203580 or 40 μM SB202190 for 30 min at 37 °C, and were then stimulated with the optimal concentrations of EGCG, VP16 or TNF (as above) for 4 h. At the end of the incubation, cells were observed under an inverted microscope. Phase-contrast micrographs are shown and the white arrows represent apoptotic cells. Original magnification, $\times$ 200. (**D**) U937 cells were preincubated with 2 μM SB203580 or 40 μM SB202190 for 30 min at 37 °C, and were then stimulated with the optimal concentrations of EGCG, VP16 or TNF (as above) for 4 h. Activations of caspase-3 and caspase-9 were evaluated by Western blotting using anti-caspase-3, anti-procaspase-9 and anti-cleaved-caspase-9 antibodies. (**E**) U937 cells were preincubated with 50 μM SP600125 for 30 min at 37 °C, and were then stimulated with the optimal concentrations of EGCG, VP16 or TNF (as above) for 4 h. Apoptosis of U937 cells was determined using the annexin V method. Representative data from three independent experiments are shown, expressed as means $\pm$ S.D. from three determinations.

same findings were obtained in OCI-AML1a cells, except that the activation of JNK but not p38 was observed at lower concentrations of EGCG in this cell line (Figure 2A, right-hand panel), which resulted in a similar dose-dependency of apoptosis for JNK but not p38. Among a panel of catechin derivatives, EGC and EGCG induced noticeable activation of JNK and p38, but (+)-catechin, EC and ECG did not (Figure 2B). The ECG-induced marginal activation of p38 but not JNK (Figure 2B) was reproducible. This structure–activity relationship of JNK/p38 (particularly p38) activation is in parallel with that of apoptosis [6]. The optimal concentrations of EGCG as well as VP16 and TNF induced time-dependent activations of JNK and p38 in U937 cells, although the time courses were different according to the stimuli and kinases (Figure 2C). EGCG rapidly and transiently induced the activation of JNK, whereas VP16 and TNF induced JNK activation for prolonged times in a biphasic manner (Figure 2C, left-hand panel). On the other hand, EGCG and TNF rapidly and persistently induced activation of p38 in a biphasic manner, whereas with VP16 p38 activation was delayed (Figure 2C, right-hand panel). Thus, in U937 cells, EGCG induced a transient activation of JNK versus the sustained and biphasic activation of p38. On the other hand in OCI-AML1a

cells, EGCG induced a sustained and biphasic activation of both JNK and p38 (Figure 2D).

Involvement of JNK and p38 during apoptosis induction and caspase activation by EGCG in U937 and OCI-AML1a cells

Data in Figures 1 and 2 suggest the possible involvement of JNK and/or p38 in the signalling pathway for apoptosis in human leukaemic cells stimulated by EGCG as well as the other two typical death agonists. Therefore, we investigated the effects of two inhibitors SB203580 and SB202190 on apoptosis of U937 cells. SB203580, a highly specific inhibitor of p38 [29], was used at a low concentration (2 μM) to assure its specificity. In fact, lower concentrations of SB203580 effectively inhibited the DNA fragmentation induced by EGCG in U937 cells (Figure 3A). On the other hand, SB202190, a rather broad inhibitor that is thought to act not only on p38 but also on JNK [30,31], was used at a relatively high concentration (40 μM). As shown in Figure 3(B) (upper panel), a high concentration of SB202190 potently inhibited the EGCG-induced DNA fragmentation in U937 cells. SB202190 also completely abolished VP16-induced DNA fragmentation, whereas SB203580 had no effect (Figure 3B, upper panel). Interestingly, neither SB203580 nor SB202190 inhibited the TNF-induced DNA fragmentation (Figure 3B, upper panel). These findings for the effects of both inhibitors on DNA fragmentation in U937 cells were confirmed by examining the apoptotic morphology of the cells under the inverted microscope (Figure 3C). SB202190 only slightly but reproducibly potentiated the DNA fragmentation and morphological changes induced by TNF (Figures 3B and 3C). Thus, in U937 cells, both inhibitors suppressed EGCG-induced apoptosis but only SB202190 suppressed VP16-induced apoptosis, and neither suppressed TNF-induced apoptosis. In OCI-AML1a cells, we observed very similar effects of SB203580 and SB202190 on apoptosis as in U937 cells (Figure 3B, lower panel) except that the EGCG-induced DNA fragmentation was resistant to the low concentration of SB203580, suggesting a less significant role for p38 during EGCG-induced apoptosis in this cell line. A high concentration of SB202190 slightly enhanced TNF-induced DNA fragmentation in this cell line (Figure 3B, lower panel). All these findings for OCI-AML1a cells were confirmed by morphological examination of the cells (results not shown).

The inhibitory effects of SB203580 and SB202190 on EGCG-induced DNA fragmentation (Figures 3A and 3B) suggest the involvement of caspase-3 distal to p38 and/or JNK in the signalling cascade of EGCG, since the DNase responsible for DNA fragmentation has been reported to be activated directly by caspase-3 [9–11]. As shown in Figure 3(D), both inhibitors almost completely abolished cleavage of caspase-3 induced by EGCG. Consistent with the findings for DNA fragmentation, SB202190 but not SB203580 inhibited VP16-induced caspase-3 cleavage, and both inhibitors enhanced rather than suppressed TNF-induced caspase-3 cleavage. Among the initiator caspases linked to caspase-3, we next studied the possible involvement of caspase-9, a caspase utilized in the post-mitochondrial pathway [32]. In accordance with the apoptosis execution (Figures 3A–3C) and caspase-3 cleavage (Figure 3D), EGCG-induced cleavage of caspase-9 at the Apaf-1 autoactivation site was almost completely abolished by both SB203580 and SB202190, whereas VP16-induced caspase-9 cleavage was inhibited only by the latter (Figure 3D). TNF-induced cleavage of caspase-9 was not inhibited by either but rather enhanced by both (Figure 3D). Thus, caspase-9 and caspase-3 are thought to be located at the position distal to JNK/p38 in the signalling cascade of EGCG.

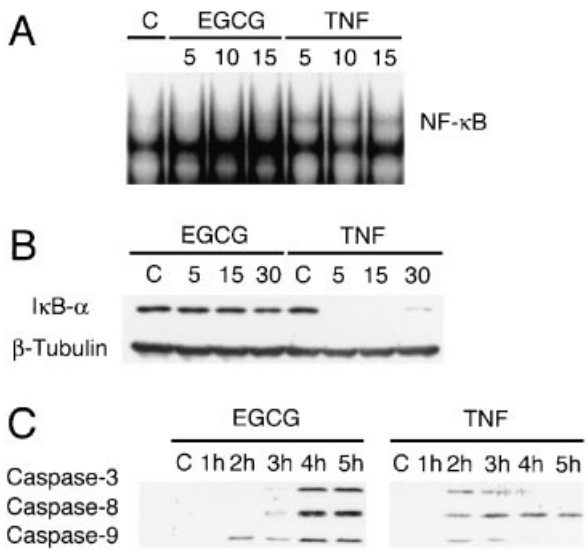

Figure 4 Activation of NF-κB and caspase-8 in U937 cells

(**A**) U937 cells were stimulated with the optimal concentrations of EGCG (400 μM) or TNF (100 ng/ml) for the indicated periods (5, 10 and 15 min) at 37 °C, and then solubilized. Electrophoretic mobility shift assays were performed using a specific oligonucleotide probe for NF-κB. C, control. (**B**) U937 cells were stimulated with the optimal concentrations of EGCG or TNF (as above) for the indicated periods (5, 15 and 30 min) at 37 °C, and then solubilized. Degradation of IκB-α was evaluated by Western blotting using anti-IκB-α antibody. Western blotting for β-tubulin is presented to show equal loading in each lane. (**C**) U937 cells were stimulated with the optimal concentrations of EGCG or TNF (as above) for the indicated periods (1–5 h) at 37 °C, and then solubilized. Activation of caspase-9, caspase-3 and caspase-8 was evaluated by Western blotting.

Data in Figures 3(A)–3(D) suggest that EGCG mainly utilizes p38 whereas VP16 mainly utilizes JNK to induce apoptosis in U937 cells. In contrast, inhibition of the JNK/p38 pathway did not inhibit but rather potentiated TNF-induced apoptotic responses. To confirm these findings, we determined the effects of SP600125, a specific inhibitor of JNK [19], on apoptosis in U937 cells. As shown in Figure 3(E), SP600125 did not inhibit EGCG-induced apoptosis under the condition that it potently suppressed VP16-induced apoptosis. In addition, SP600125 enhanced TNF-induced apoptosis (Figure 3E).

Effect of EGCG on NF-κB and caspase-8 in U937 cells

EGCG induced the activation of p38 in an almost identical time course with TNF (Figure 2C), suggesting a possibility that EGCG induces apoptosis of the cells via a specific death receptor-like pathway. To explore this hypothesis, we studied the effects of EGCG on NF-κB in comparison with TNF. As shown in Figure 4(A), EGCG did not induce activation of NF-κB under the same conditions in which TNF did, as determined by electrophoretic mobility shift assay. To further confirm this, we determined degradation of IκB-α, the essential upstream signalling event of NF-κB activation [33]. As shown in Figure 4(B), EGCG did not induce degradation of NF-κB under the same conditions in which TNF potently did this.

Not only TNF but also EGCG induced cleavage of caspase-8 in addition to caspase-9 and caspase-3 (Figure 4C). However, the time courses of caspase cleavage were distinct for EGCG and TNF; that is, EGCG rapidly induced caspase-9 followed by the other two caspases whereas TNF induced three caspases rapidly and almost simultaneously, suggesting that EGCG-

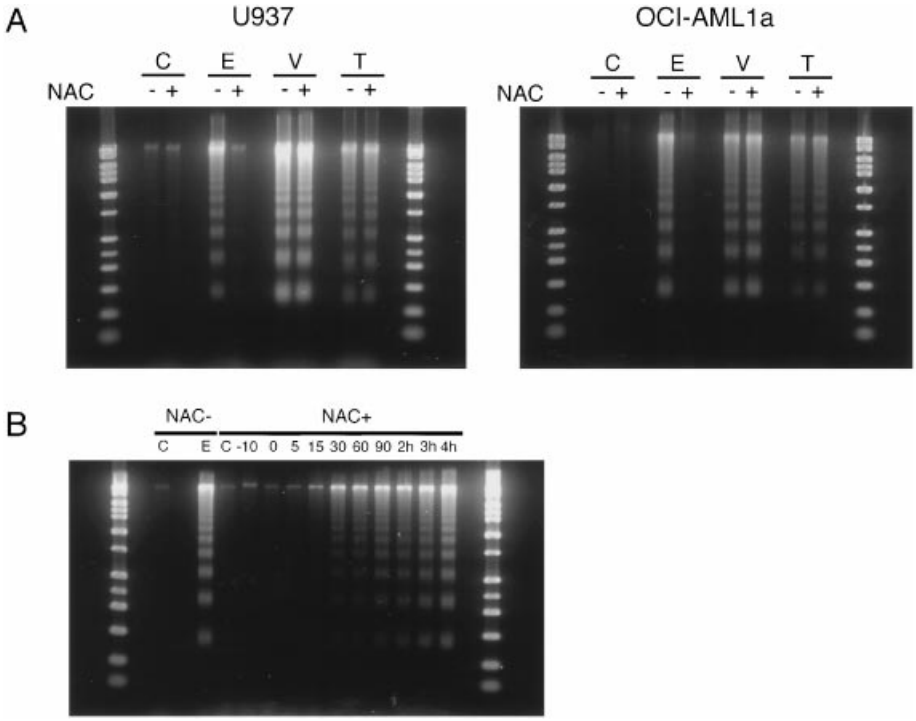

Figure 5 Effects of NAC on DNA fragmentation in U937 and OCI-AML1a cells stimulated by EGCG, VP16 and TNF

(**A**) U937 (left-hand panel) and OCI-AML1a cells (right-hand panel) were preincubated with 5 mM NAC for 15 min at 37 °C, and were then stimulated with the optimal concentrations of EGCG (400 μM for U937 cells and 200 μM for OCI-AML1a cells), VP16 (10 μg/ml) or TNF (100 ng/ml) for 4 h at 37 °C. (**B**) NAC (5 mM) was added to the culture of U937 cells either before or after the addition of 400 μM EGCG. The total incubation period with EGCG was always 4 h, and the timing of NAC addition with respect to EGCG addition is indicated. The presence of internucleosomal DNA fragmentation was examined by agarose gel electrophoresis. C, control; E, EGCG; V, VP16; T, TNF.

induced cleavage of caspase-8 might result from the activation of caspase-9 and caspase-3, as has been reported by others [34].

Effects of NAC on apoptosis of U937 and OCI-AML1a cells

Redox and/or ROS are known to play an important role in the intracellular signalling pathway of apoptosis [35,36]. To address their involvement in the EGCG signalling pathway, we studied the effects of NAC, a reducing agent and a scavenger of ROS [35,36], on apoptosis induced by EGCG in comparison with VP16 and TNF. Preincubation of U937 cells with the optimal concentration of NAC (5 mM) for 10 min almost completely suppressed DNA fragmentation (Figure 5A, left-hand panel) in U937 cells stimulated by EGCG. In contrast, NAC preincubation failed to inhibit apoptosis induced by VP16 and TNF (Figure 5A, left-hand panel). These findings for DNA fragmentation were confirmed by morphological examinations using a microscope (results not shown). In another human leukaemic cell line, OCI-AML1a, an almost identical phenomenon was observed; that is, NAC exerted a potent inhibitory effect on EGCG-induced apoptosis but had no effect on VP16- or TNF-induced apoptosis (Figure 5A, right-hand panel). The inhibitory effect of NAC on EGCG-induced apoptosis was observed even when EGCG and NAC were added to U937 cells simultaneously and when NAC was added to the cells after 5 min of catechin stimulation (Figure 5B). However, the inhibition was attenuated when the addition of NAC was delayed by 15 min to 2 h and after a delay of 3–4 h the NAC was unable to inhibit apoptosis (Figure 5B), suggesting the involvement of an intracellular target for NAC at an early step during apoptosis signalling of EGCG.

Effects of NAC on the activation of JNK and p38 in U937 and OCI-AML1a cells

Results in Figures 2, 3 and 5 clearly show that both JNK/p38 and NAC targets are essential for EGCG-induced apoptosis, although the causal relationship between JNK/p38 and NAC target is unclear. Therefore, we evaluated the possible roles of a NAC target in the activation of JNK and p38. As shown in Figure 6(A), NAC almost completely abolished the time-dependent activation of JNK and p38 in both U937 and OCI-AML1a cells stimulated by EGCG. We then compared the effects of NAC on the activation of JNK and p38 with various apoptosis-inducing stimuli in both cell lines (Figure 6B). Under the conditions in which EGCG-induced activation of JNK and p38 was completely abolished, NAC had no effect on VP16-induced activation of JNK and p38 in either U937 or OCI-AML1a cells (Figure 6B). The TNF-induced activation of JNK and p38 was only partially but reproducibly inhibited by NAC (Figure 6B).

Characterization of the effects of NAC on EGCG-induced events

To extend the effects of NAC on EGCG-induced apoptosis and rule out the direct action of NAC on EGCG itself, we performed

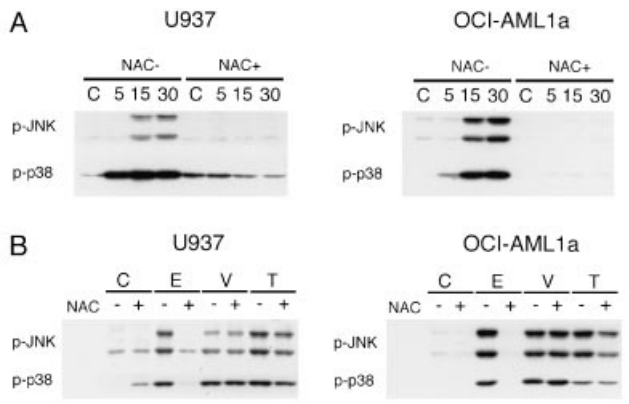

Figure 6 Effects of NAC on the activation of JNK and p38 in U937 and OCI-AML1a cells stimulated by EGCG, VP16 and TNF

(**A**) U937 (left-hand panel) and OCI-AML1a cells (right-hand panel) were preincubated with 5 mM NAC for 15 min at 37 °C, and were then stimulated with 400 μM (for U937 cells) or 200 μM (for OCI-AML1a cells) EGCG for the indicated periods (5, 15 and 30 min) at 37 °C. (**B**) U937 (left-hand panel) and OCI-AML1a cells (right-hand panel) were preincubated with 5 mM NAC for 15 min at 37 °C, and were then stimulated with the optimal concentrations of EGCG (400 μM for U937 cells and 200 μM for OCI-AML1a cells), VP16 (10 μg/ml) or TNF (100 ng/ml) for 30 min at 37 °C. Activation states of JNK and p38 were evaluated by Western blotting using antibodies specific for phosphorylated and activated forms of JNK and p38, respectively. C, control; E, EGCG; V, VP16; T, TNF.

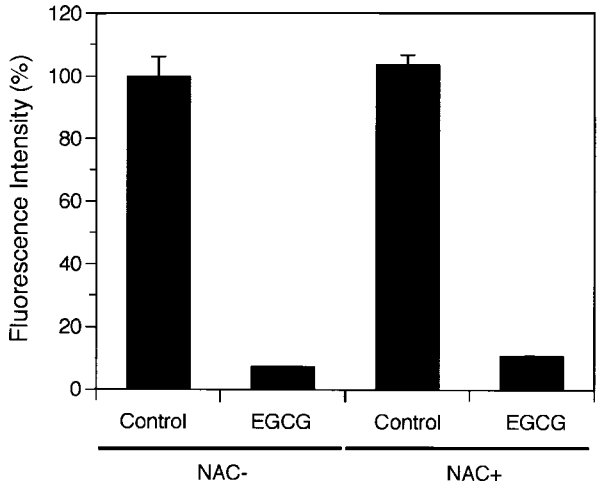

Figure 8 Effects of NAC and EGCG on urokinase activity

Urokinase was preincubated with 400 μM EGCG in the presence or absence of 5 mM NAC, and were then incubated with the fluorescent peptide substrate Glt-Gly-Arg-MCA for 1 h at 37 °C. Cleavage of peptide substrate as determined by release of MCA was measured by a fluorescence spectrophotometer. The results are expressed as a percentage of the control (urokinase activity without NAC or EGCG). Representative data from three independent experiments are shown, with means ± S.D. from three determinations.

additional two experiments. First, we determined the effect of DTT, another reducing agent structurally unrelated to NAC, on EGCG-induced apoptosis and JNK/p38 activation. As shown in Figure 7, DTT exerted potent inhibitory effects, which were comparable with those of NAC, on apoptosis and JNK/p38 in U937 and OCI-AML1a cells. Secondly, we studied whether NAC might directly affect EGCG using a cell-free assay system. It has been reported that EGCG inhibits urokinase activity *in vitro* [37], and we confirmed this phenomenon (Figure 8). By

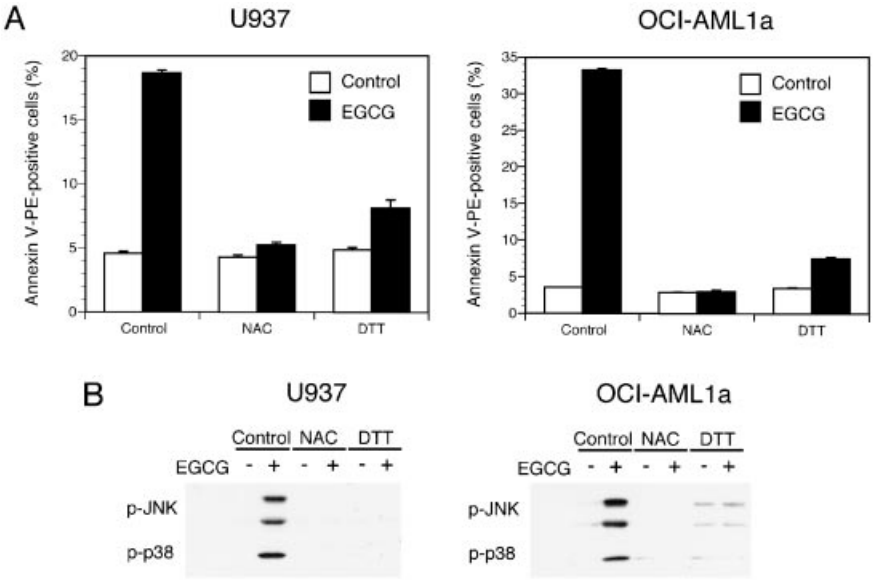

Figure 7 Effects of NAC and DTT on apoptosis and the activation of JNK and p38 in U937 and OCI-AML1a cells stimulated by EGCG

(**A**) U937 (left-hand panel) and OCI-AML1a cells (right-hand panel) were preincubated with 5 mM NAC or 500 μM DTT for 15 min at 37 °C, and were then stimulated with the optimal concentrations of EGCG (400 μM for U937 cells and 200 μM for OCI-AML1a cells) for 4 h at 37 °C. Apoptosis of the cells was determined using the annexin V method. Representative data from three independent experiments are shown, with means ± S.D. from three determinations. (**B**) U937 (left-hand panel) and OCI-AML1a cells (right-hand panel) were preincubated with 5 mM NAC or 500 μM DTT for 15 min at 37 °C, and were then stimulated with the optimal concentrations of EGCG (400 μM for U937 cells and 200 μM for OCI-AML1a cells) for 30 min at 37 °C. Activation states of JNK and p38 were evaluated by Western blotting using antibodies specific for phosphorylated and activated forms of JNK and p38.

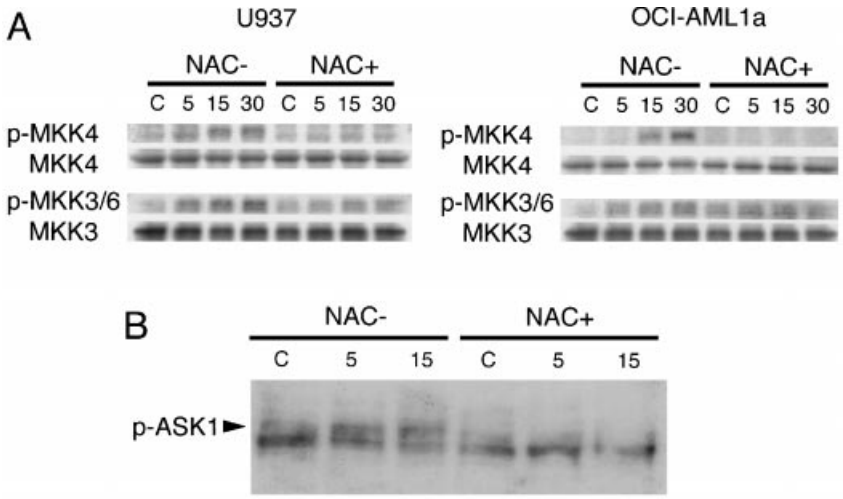

Figure 9 Effects of NAC on the activation of MKK4, MKK3/6 and ASK1 in U937 and OCI-AML1a cells stimulated by EGCG

(**A**) U937 and OCI-AML1a cells were preincubated with 5 mM NAC for 15 min at 37 °C, and then stimulated with the optimal concentrations of EGCG (400 μM for U937 cells and 200 μM for OCI-AML1a cells) for the indicated periods (5, 15 and 30 min) at 37 °C. Activation states of MKK4 and MKK3/6 were evaluated by Western blotting using antibodies specific for phosphorylated and activated forms of MKK4 and MKK3/6, respectively. (**B**) U937 cells were preincubated with 5 mM NAC for 15 min at 37 °C, and were then stimulated with 400 μM EGCG for the indicated periods (5 and 15 min) at 37 °C. Activation state of ASK1 was evaluated by Western blotting using an antibody specific for the phosphorylated and activated form of ASK1. The upper band of the doublet represents the phosphorylated ASK1. C, control.

using this assay system, we found that NAC had no effect on the inhibitory action of EGCG against urokinase (Figure 8).

Involvement of the upstream signalling molecules of JNK and/or p38 in EGCG-stimulated cells and the effects of NAC on them

To determine the level of the NAC target in the JNK/p38 pathway, we investigated the effects of NAC on upstream signalling molecules of JNK/p38 including MKK4 and MKK3/6, as well as ASK1 in human U937 and OCI-AML1a cells stimulated by EGCG, using the specific antibodies that recognize phosphorylated and activated forms of these upstream kinases. As shown in Figure 9(A), EGCG induced the activation of both MKK4 and MKK3/6 in a time-dependent manner. Under the same conditions, NAC potently inhibited EGCG-induced activation of both MKK4 and MKK3/6. Thus, the NAC target lies upstream of MKK4 and MKK3/6. Next, we evaluated the effect of NAC on the activation of ASK1, one of the upstream kinases which activate MKK4 and MKK3/6. As shown in Figure 9(B), EGCG induced the activation of ASK1, which was potently inhibited by NAC, suggesting that a NAC target lies upstream of ASK1.

To further confirm the involvement of p38 and JNK and determine the involvement of MKKs and ASK1 during EGCG-induced apoptosis, we investigated the effects of dominant negative mutants of JNK1, MKK4, MKK7, MKK6 and ASK1 on EGCG-induced apoptosis in U937 and OCI-AML1a cells. As shown in Figure 10 (upper panel), EGCG-induced cell death as determined by PI positivity in U937 cells was not affected by control gene transfection, but was potently inhibited by the transfection of dominant negative ASK1, MKK6, MKK4 and JNK1. Dominant negative MKK7 did not exert significant effects on EGCG-induced cell death in this cell line (Figure 10, upper panel). On the other hand, all of the dominant negative mutants, including dominant negative MKK7, inhibited EGCG-induced cell death in OCI-AML1a cells (Figure 10, lower panel). These findings further confirm the potential role of the ASK1/MKK/JNK/p38 cascade in EGCG-induced apoptosis in human leukaemic cells. No effect of dominant negative MKK7 (Figure 10, upper panel) might reflect the findings in Figure 3, which shows the major role of p38 rather than JNK, at least in U937 cells stimulated by EGCG.

Effects of EGCG on the ROS level and redox status in cells

A recent study clarified the involvement of ROS and redox-related mechanisms in the activation of the ASK1 pathway [18,36]. In addition, the present study showed that NAC and DTT, reducing agents and ROS scavengers, potently inhibited ASK1/MKK/JNK/p38 activation as well as the apoptosis induced by EGCG (Figures 5–7 and 9), suggesting the existence of a specific target for NAC and DTT upstream to the apoptosis-executing MAP kinases in the EGCG-activated signalling pathway. To address these problems, we studied whether EGCG really generates intracellular ROS and/or exerts some effects on the intracellular redox state in human leukaemic cells. In addition, we investigated whether NAC could affect these EGCG-induced oxidative responses. As shown in Figure 11(A), EGCG, but not VP16 and TNF, up-regulated the intracellular level of ROS in U937 cells, although the potency was much less than that of H_2O_2, the positive control. Interestingly, the combined stimulation of U937 cells with EGCG plus H_2O_2 produced much less intracellular ROS than H_2O_2 alone (Figure 11A). The increase of intracellular ROS by EGCG and/or H_2O_2 was almost completely abolished by NAC (Figure 11A). To rule out the non-specific inhibitory effects of p38/JNK inhibitors on intracellular ROS, we then determined the effects of SB203580 and SB202190 on EGCG-induced increase of intracellular ROS in U937 cells. Neither inhibitor had any significant effects on EGCG-induced ROS (EGCG alone, 2.3 ± 0.2; EGCG + SB203580, 2.3 ± 0.1; EGCG + SB202190, 2.4 ± 0.2; data are expressed as fold increase over the control cells, means $\pm$ S.D. from three determinations).

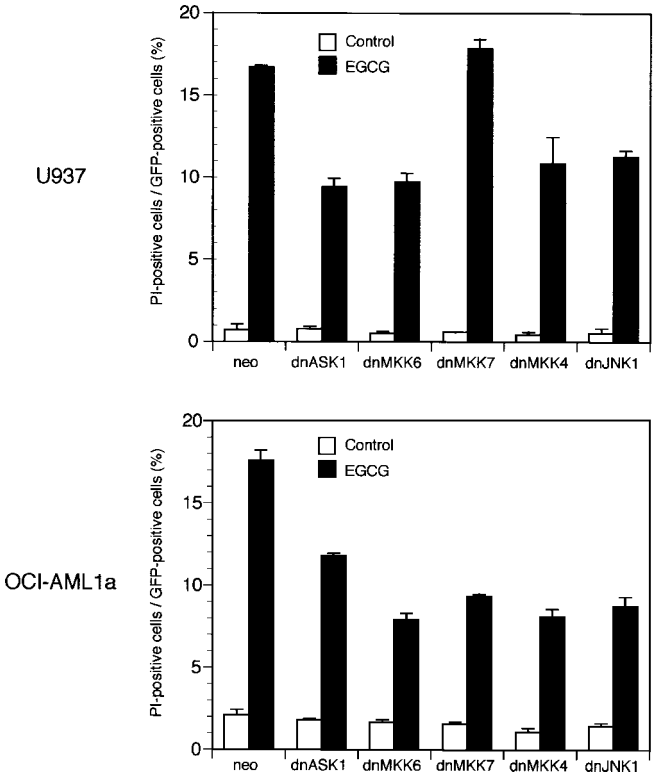

Figure 10 Effects of dominant negative JNK, MKKs and ASK1 on U937 cells stimulated by EGCG

The GFP expression vector and pCI-neo (control) or expression vectors for dominant negative (dn) mutants were co-transfected into U937 (upper panel) and OCI-AML1a cells (lower panel) using Nucleofector technology. Transfected cells were stimulated with (EGCG) or without (Control) the optimal concentrations of EGCG (400 μM for U937 cells and 200 μM for OCI-AML1a cells) for 4 h at 37 °C, and were then suspended in staining buffer containing 1 μg/ml PI. The two-colour analyses (GFP and PI) were performed using FACS Calibur. Only GFP-positive transduced cells were counted for PI positivity, and the quantity of dead cells was expressed as percentage of PI-positive cells in the GFP-positive cells. Transfection efficiency (GFP-positive cells/total cells) was approx. 30–40% in U937 cells and 60–80% in OCI-AML1a cells in this system. Representative data from three independent experiments are shown, with means $\pm$ S.D. from three determinations. neo, pCI-neo-transfected cells.

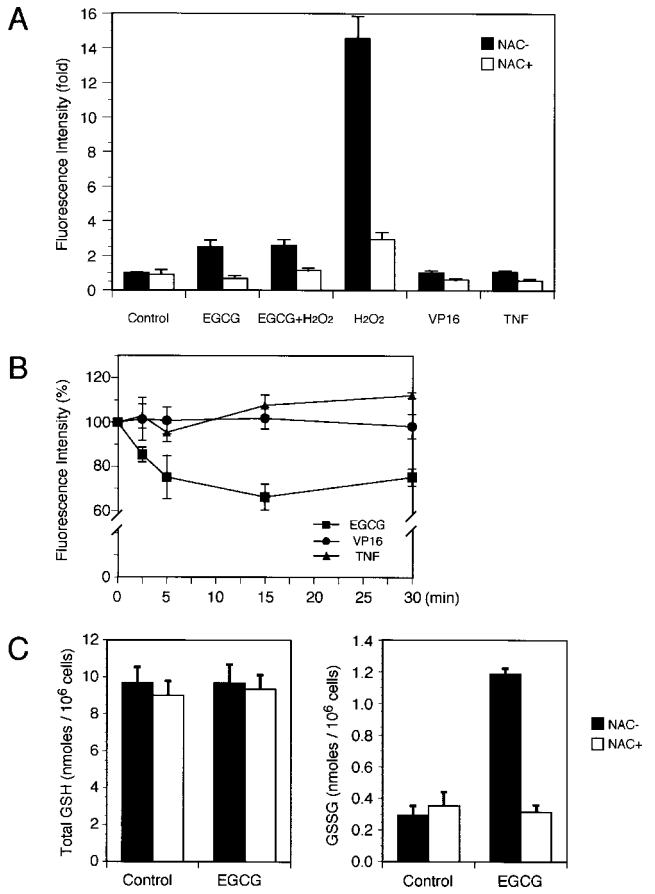

Figure 11 Intracellular concentrations of ROS and GSH in U937 cells stimulated by EGCG

(**A**) U937 cells were preincubated with or without 5 mM NAC for 15 min at 37 °C, and then stimulated with 400 μM EGCG, 1 mM H_2O_2, a combination of both, 10 μg/ml VP16 or 100 ng/ml TNF for 15 min at 37 °C. Intracellular ROS concentration was measured using DCFH-DA as a probe, and the results were expressed as fold increase over control cells. (**B**) U937 cells were stimulated with 400 μM EGCG (■), 10 μg/ml VP16 (●) or 100 ng/ml TNF (▲) for the indicated periods at 37 °C. Relative levels of intracellular GSH were measured by the ApoAlert® Glutathione Detection Kit using monochlorobimane as a probe, and the results were expressed as a percentage of the control cells. (**C**) U937 cells were preincubated with or without 5 mM NAC for 15 min at 37 °C, and were then stimulated with 400 μM EGCG for 15 min at 37 °C. Intracellular concentrations of total GSH (left-hand panel) and GSSG (right-hand panel) were measured by the Bioxytech® GSH/GSSG-412™ kit using 5,5′-dithiobis-2-nitrobenzoic acid as a chromogen. In all panels, representative data from three independent experiments are shown, with means $\pm$ S.D. from three determinations.

As a parameter of the intracellular redox state, we determined the intracellular concentrations of GSH, the most abundant redox-regulating molecule in cells [38]. As shown in Figure 11(B), EGCG induced a time-dependent decrease of intracellular GSH in U937 cells as determined by the Clontech method using monochlorobimane as a probe. This effect of EGCG was very rapid, and a significant ($P < 0.01$) decrease was observed even at 2.5 min. Under the same conditions, VP16 and TNF exerted no or minimal effects on intracellular GSH in U937 cells (Figure 11B). To quantify more precisely the intracellular level of both total and oxidized GSH and to evaluate the effects of NAC on them, we used an additional assay system (from OXIS). The total GSH level was not affected by EGCG (Figure 11C, left-hand panel), although GSSG was increased by EGCG (Figure 11C, right-hand panel), indicating an EGCG-induced net decrease in reduced GSH. The relative amount of reduced GSH in EGCG-treated cells determined by the OXIS method was roughly estimated by subtracting twice the level of GSSG from the total amount of GSH, and it was found to be approx. 70–80% that of control cells, a finding consistent with that from the Clontech method (Figure 11B). The increase in GSSG was almost completely abolished by NAC (Figure 11C, right-hand panel).

To confirm the intracellular roles of GSH, we investigated the effect of the decrease in intracellular GSH on EGCG-induced apoptosis. When U937 and OCI-AML1a cells were pretreated with 1 mM BSO, a inhibitor of GSH synthesis [39,40], for 10 h, the intracellular levels of GSH were decreased to $71 \pm 3\%$ and $61 \pm 1\%$ of non-pretreated control cells, respectively (Figure 12A). Under the same conditions, EGCG-induced apoptosis as determined by annexin V positivity in these U937 and OCI-AML1a cells was markedly potentiated (Figure 12B). These findings together indicate that EGCG induces NAC-sensitive intracellular oxidative stress at an early step in the apoptosis pathway.

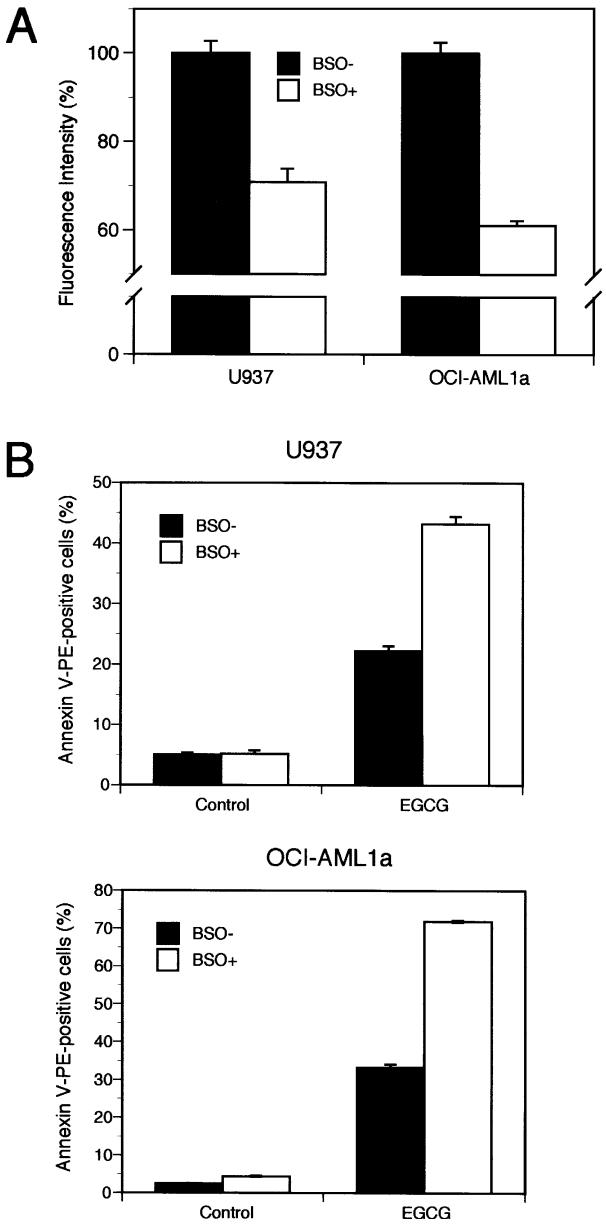

Figure 12 Effects of BSO on GSH and apoptosis in U937 and OCI-AML1a cells stimulated by EGCG

(**A**) U937 and OCI-AML1a cells were incubated with or without 1 mM BSO for 10 h at 37 °C. Relative levels of intracellular GSH were measured by the ApoAlert® Glutathione Detection Kit using monochlorobimane as a probe, and the results were expressed as a percentage of the control cells. (**B**) U937 (top panel) and OCI-AML1a cells (bottom panel) were preincubated with 1 mM BSO for 10 h at 37 °C, and were then stimulated with the optimal concentrations of EGCG (400 μM for U937 cells and 200 μM for OCI-AML1a cells) for 4 h at 37 °C. Apoptosis of the cells was determined using the annexin V method. Representative data from three independent experiments are shown, with means $\pm$ S.D. from three determinations.

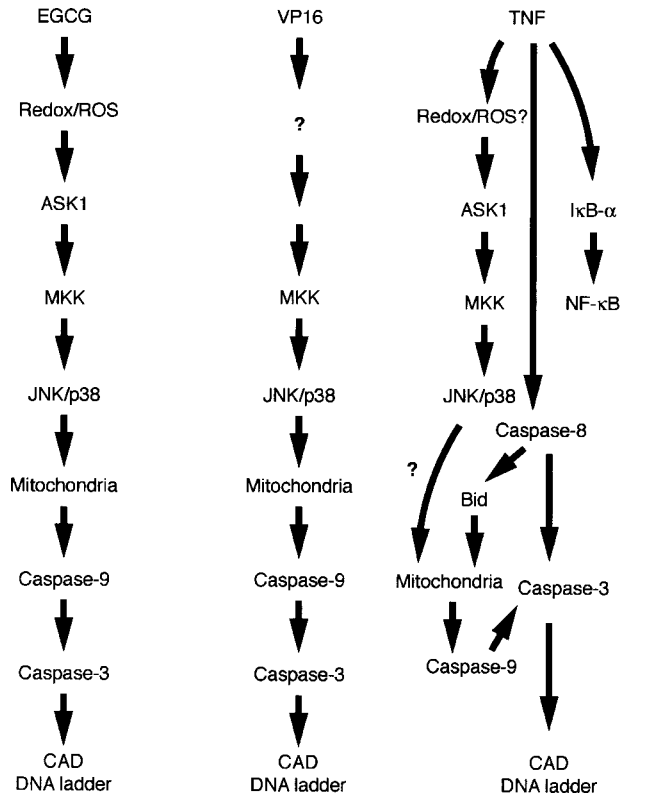

Scheme 1 Intracellular signalling pathways for apoptosis in human leukaemic cells stimulated by EGCG as compared with those induced by VP16 and TNF

Intracellular signal transduction pathways of EGCG resulting in DNA fragmentation of cells are shown compared with those of VP16 and TNF. The redox/ROS system and JNK/p38 cascade play essential and central roles in the EGCG apoptotic pathways.

DISCUSSION

The present results show that EGCG induces activation of the JNK/p38 pathway via an intracellular target for NAC and DTT (Figures 6 and 7) and that the activation of JNK/p38 by EGCG was linked to the activation and/or cleavage of caspases as well as the execution of apoptosis (Figures 3 and 10) in human leukaemic cells. In contrast, VP16-induced activation of JNK/p38 did not seem to be mediated by a NAC target (Figure 6B), although the activation of JNK/p38 did lead to caspase activation and apoptosis in VP16-stimulated cells (Figure 3). In TNF-stimulated cells, JNK/p38 may not be responsible for caspase activation and may not be essential or a prerequisite for apoptosis (Figure 3) [41]. It is also possible that JNK/p38 is to some extent linked to apoptosis in the TNF pathway, although apoptosis by this pathway is effectively executed even in the presence of JNK/p38 inhibitors (Figures 3B, 3C and 3E) via another independent pathway (probably the caspase-8 cascade initiated by the TNF receptor) [41]. The partial involvement of a NAC target for JNK/p38 activation by TNF was suggested (Figure 6B), although TNF-induced JNK/p38 activation was fundamentally resistant to NAC at least in our experimental system (Figure 6B). Such a NAC-resistant pathway for TNF to induce JNK/p38 activation might be provoked by the direct interaction between TNF receptor-associated factor 2 [41] and MAP kinase cascade via an unknown non-redox mechanism. The hypotheses based on the findings obtained in this study and the results of previous observations [7,10,17,32,41] are summarized in Scheme 1. Thus, the essential roles of JNK and/or p38 during the apoptotic processes of both EGCG and VP16 suggest that EGCG utilizes the apoptotic signalling pathway of the toxic agent (or chemically induced) type rather than that of the death receptor (or receptor-induced) type, although the

NAC target lies only in the upstream pathway of EGCG. On the other hand, the signalling pathway utilized by EGCG partly resembles that by TNF since both EGCG and TNF induced a rapid and persistent activation of p38 with almost identical time courses (Figure 2C, right-hand panel) as well as significantly utilizing the NAC target to activate p38 (Figure 6B). In addition, EGCG and TNF showed a similar pattern of cell cycle distribution (Figure 1E). However, TNF but not EGCG provoked activation of NF-κB (Figures 4A and 4B), a well-known transcription factor that generates the survival signal [41], and EGCG- but not TNF-induced primary activation of caspase-9 (Figure 4C).

In the situations when both JNK and p38 were activated, we were interested in which of them was more important for the execution of apoptosis. Several interesting findings for this problem were obtained in this study. For example, a low concentration of SB203580, which is hypothesized to inhibit p38 but not JNK, sufficiently suppressed caspase activation and apoptosis induced by EGCG in U937 cells. In contrast, VP16-induced caspase activation and apoptosis were suppressed only by the high concentration of SB202190, which is a rather broad inhibitor of both JNK and p38, but not by the low concentration of SB203580 (Figure 3). In addition, SP600125, a specific inhibitor of JNK, did not inhibit EGCG-induced apoptosis under the conditions in which it potently suppressed VP16-induced apoptosis (Figure 3E). These findings for U937 cells suggest that EGCG activated the caspase cascade and apoptosis mainly via p38 rather than JNK while the VP16 activations were mainly via JNK, in spite of the fact that both agents induced activation of both kinases. A greater role for p38 than JNK in EGCG-induced apoptosis in U937 cells was also suggested by the experiment using dominant negative mutant genes of the JNK/p38 pathway (Figure 8).

Activation of JNK/p38 is not always associated with apoptosis, and might play important roles in cell survival and/or differentiation [42–44]. In this study, we also observed that inhibition of JNK/p38 did not inhibit but rather enhanced apoptosis and caspase activation in human leukaemic cells stimulated by TNF (Figure 3), suggesting that the survival signal was generated by JNK/p38 in this situation. At present, it is not completely clear why the same kinase signal provokes the opposite effects downstream which determine cell survival or death. One attractive hypothesis is that the duration of JNK/p38 activation is a critical point for these phenomena; that is, transient activation contributes to cell survival whereas a sustained (and biphasic) activation induces cell death [45]. In this context, the transient activation of JNK versus the sustained activation of p38 in U937 cells stimulated by EGCG are of interest, since EGCG was thought to induce apoptosis mainly via p38 in this cell line, as described above. In contrast to U937 cells, EGCG induced sustained and biphasic activation of JNK (Figure 2D) and the dose–response curve for apoptosis paralleled that for JNK activation but not for p38 activation (Figure 2A, right-hand panel) in OCI-AML1a cells. In addition, EGCG-induced apoptosis in OCI-AML1a cells, unlike that in U937 cells, was resistant to a p38 inhibitor but was sensitive to a broad inhibitor of both JNK and p38 (Figure 3B, lower panel). These findings suggest that EGCG executed apoptosis mainly via the prolonged and biphasic activation of JNK at least in OCI-AML1a cells.

It has already been reported that EGCG induces the activation of caspase-3-like activity and that a broad caspase inhibitor (z-VAD-FMK; carbobenzoxy-Val-Ala-Asp-fluoromethylketone) as well as a caspase-3 inhibitor (DEVD-CHO; Asp-Glu-Val-Asp-aldehyde) potently inhibit EGCG-induced apoptosis in human chondrosarcoma cells [16]. We also confirmed some of these findings using another caspase inhibitor {z-Asp-CH_2-DCB; carbobenzoxy-Asp-CH_2-[(2,6-dichlorobenzoyl)oxy]methane} and human leukaemic cells [6]. In the present study, we showed that EGCG induced the cleaved and activated form of caspase-3 (Figures 3D and 4C). In addition, we observed that caspase-9 and caspase-3 were located downstream of JNK/p38 in EGCG-stimulated U937 cells (Figure 3D). In regard to how the cellular stress activates caspase-3, several recent reports have shown the involvement of the JNK/p38 (and ASK1) pathway upstream to the caspase cascade [12–15]. According to these reports, activated JNK/p38 affects the mitochondrial pathway, including cytochrome *c*/Apaf-1/caspase-9 via a caspase-independent unknown mechanism, and the activation of these mitochondrial pathways results in the activation of caspase-3 and CAD leading to DNA fragmentation. These phenomena seem to be applicable to the EGCG pathway, although an intervening molecule between JNK/p38 and the mitochondria remains to be determined. A member of the apoptosis-inducing Bcl-2 family, such as Bax, has recently been proposed as a candidate for such a molecule [14]. More recently, phosphorylation of Bcl-2 by p38 has been reported to trigger mitochondrial pathways [46].

In the present study, we cannot exactly identify the most proximal molecular event initiated by EGCG and the initial target of NAC that lies upstream of ASK1. ROS is known to play a critical role in some situations of apoptosis [18,35,36], and EGCG did induce a detectable level of intracellular ROS, at least in human leukaemic cells (Figure 11A). Alternatively, EGCG might shift the intracellular redox balance towards oxidation, based upon the observation of an increase in oxidized GSH in EGCG-stimulated U937 cells (Figures 11B and 11C). Importantly, NAC almost completely abolished the generation of both ROS and GSSG (Figure 11) as well as activation of the JNK/p38 cascade (Figures 6, 7 and 9) and the execution of apoptosis (Figure 5A). In addition, the decrease in intracellular GSH by an inhibitor of GSH synthesis rendered U937 cells more susceptible to EGCG-induced apoptosis (Figure 12). Thus, NAC might inhibit EGCG-induced JNK/p38 activation and apoptosis by correcting the intracellular redox unbalance and/or by scavenging intracellular ROS. Among the intracellular redox molecules, thioredoxin has been reported to function as a redox-dependent regulator of the JNK/p38 pathway via direct regulation of ASK1 activity [18,36], and ASK1 was found to be involved in EGCG-induced apoptogenic pathway (Figures 9 and 10). In this context, EGCG might exert its proapoptotic effect via redox rather than ROS, and intracellular target of NAC in the present experiment would be redox that could be regulated by the intracellular concentrations of GSH, the most abundant redox-regulating molecule in cells [38].

EGCG is well known as a scavenger of ROS in extracellular environments [47,48]. This characteristic of catechin compounds might be closely related to their useful anti-carcinogenic or anti-cytotoxic activities [49,50]. In contrast, EGCG did induce intracellular production of ROS and a shift of the intracellular redox balance towards the oxidation state, as presented in Figure 11. We cannot explain these dual and opposite effects of catechin on the oxygen balance. In this study, we found that EGCG inhibited the potent increase in intracellular ROS induced by H_2O_2 (Figure 11A), suggesting that the antioxidant actions of catechins may also function within the cells. However, we observed that the inhibition of the H_2O_2-induced increase in intracellular ROS did not result in the inhibition of the H_2O_2-induced JNK/p38 activation and apoptosis at least in human leukaemic U937 cells (K. Saeki and A. Yuo, unpublished work). In contrast, EGCG potently inhibited the cytotoxicity as well as the ROS and JNK/p38 in human keratinocytes stimulated by

UV radiation [50,51]. It remains to be determined how the different mechanisms work during the antioxidant (cytoprotective) versus oxidant (cytotoxic) actions of EGCG.

We observed that EGCG but not TNF induced intracellular ROS production and GSH oxidation (Figure 11) and TNF but not EGCG induced NF-κB activation (Figure 4), at least in human leukaemic cell lines. These reciprocal findings are not consistent with previous observations, since TNF is reported to induce intracellular ROS in many cells and most agents that generate ROS tend to activate NF-κB [52–56]. In addition, some of the co-authors of this study clearly demonstrated essential roles of the NAC-sensitive ASK1 and JNK/p38 pathway during TNF-induced apoptosis in murine embryonic fibroblasts [45]. On the other hand, another group reported that the inhibition of p38 potentiated TNF-induced apoptosis in U937 cells [42], a finding consistent with the results of the present study. Thus the redundant signalling pathways for cell death and survival seem be regulated in a complex manner according to the cell type. In regard to NF-κB, a recent report shows polyphenol-induced inhibition of NF-κB activity in human cancer cell lines [57].

In this study, we clearly show that EGCG induces apoptotic cell death via three important signalling pathways, redox/ROS pathway, MAP kinase pathway and caspase pathway, which are triggered by EGCG in this sequence. The causal relationships between these three sequential pathways were strongly suggested, and a more exact identification of the intervening molecules linking the three independent pathways to one another is currently underway in our laboratory.

This work was supported in part by a Grant-in-Aid for the Second Term Comprehensive 10-year Strategy for Cancer Control from the Ministry of Health and Welfare of Japan and the O-CHA (tea) Pioneer Academic Research Grant Program from Shizuoka Prefectural Government. We thank Professor Eisuke Nishida, Professor Fuyuki Ishikawa, Dr Chifumi Kitanaka and Dr Hiroyuki Seimiya for providing dominant negative MKK6, MKK7 and JNK1. We also thank Dr Brydon L. Bennett for providing SP600125.

REFERENCES

1 Fujiki, H., Yoshizawa, S., Horiuchi, T., Suganuma, M., Yatsunami, J., Nishiwaki, S., Okabe, S., Nishiwaki-Matsushima, R., Okuda, T. and Sugimura, T. (1992) Anticarcinogenic effects of (−)-epigallocatechin gallate. Prev. Med. **21**, 503–509

2 Yamane, T., Takahashi, T., Kuwata, K., Oya, K., Inagake, M., Kitao, Y., Suganuma, M. and Fujiki, H. (1995) Inhibition of N-methyl-N′-nitro-N-nitrosoguanidine-induced carcinogenesis by (−)-epigallocatechin gallate in the rat glandular stomach. Cancer Res. **55**, 2081–2084

3 Ahmad, N., Feyes, D. K., Nieminen, A. L., Agarwal, R. and Mukhtar, H. (1997) Green tea constituent epigallocatechin-3-gallate and induction of apoptosis and cell cycle arrest in human carcinoma cells. J. Natl. Cancer Inst. **89**, 1881–1886

4 Chung, J. Y., Huang, C., Meng, X., Dong, Z. and Yang, C. S. (1999) Inhibition of activator protein 1 activity and cell growth by purified green tea and black tea polyphenols in H-ras-transformed cells: structure-activity relationship and mechanisms involved. Cancer Res. **59**, 4610–4617

5 Isemura, M., Saeki, K., Minami, T., Hayakawa, S., Kimura, T., Shoji, Y. and Sazuka, M. (1999) Inhibition of matrix metalloproteinases by tea catechins and related polyphenols. Ann. N.Y. Acad. Sci. **878**, 629–631

6 Saeki, K., Hayakawa, S., Isemura, M. and Miyase, T. (2000) Importance of a pyrogallol-type structure in catechin compounds for apoptosis-inducing activity. Phytochemistry **53**, 391–394

7 Ichijo, H. (1999) From receptors to stress-activated MAP kinases. Oncogene **18**, 6087–6093

8 Yuo, A. (2001) Differentiation, apoptosis, and function of human immature and mature myeloid cells: intracellular signalling mechanism. Int. J. Hematol. **73**, 438–452

9 Stennicke, H. R. and Salvesen, G. S. (2000) Caspases – controlling intracellular signals by protease zymogen activation. Biochim. Biophys. Acta **1477**, 299–306

10 Nagata, S. (2000) Apoptotic DNA fragmentation. Exp. Cell Res. **256**, 12–18

11 Enari, M., Sakahira, H., Yokoyama, H., Okawa, K., Iwamatsu, A. and Nagata, S. (1998) A caspase-activated DNase that degrades DNA during apoptosis, and its inhibitor ICAD. Nature (London) **391**, 43–50

12 Tournier, C., Hess, P., Yang, D. D., Xu, J., Turner, T. K., Nimnual, A., Bar-Sagi, D., Jones, S. N., Flavell, R. A. and Davis, R. J. (2000) Requirement of JNK for stress-induced activation of the cytochrome c-mediated death pathway. Science **288**, 870–874

13 Assefa, Z., Vantieghem, A., Garmyn, M., Declercq, W., Vandenabeele, P., Vandenheede, J. R., Bouillon, R., Merlevede, W. and Agostinis, P. (2000) p38 mitogen-activated protein kinase regulates a novel, caspase-independent pathway for the mitochondrial cytochrome c release in ultraviolet B radiation-induced apoptosis. J. Biol. Chem. **275**, 21416–21421

14 Ghatan, S., Larner, S., Kinoshita, Y., Hetman, M., Patel, L., Xia, Z., Youle, R. J. and Morrison, R. S. (2000) p38 MAP kinase mediates Bax translocation in nitric oxide-induced apoptosis in neurons. J. Cell Biol. **150**, 335–347

15 Hatai, T., Matsuzawa, A., Inoshita, S., Mochida, Y., Kuroda, T., Sakamaki, K., Kuida, K., Yonehara, S., Ichijo, H. and Takeda, K. (2000) Execution of apoptosis signal-regulating kinase 1 (ASK1)-induced apoptosis by the mitochondria-dependent caspase activation. J. Biol. Chem. **275**, 26576–26581

16 Islam, S., Islam, N., Kermode, T., Johnstone, B., Mukhtar, H., Moskowitz, R. W., Goldberg, V. M., Malemud, C. J. and Haqqi, T. M. (2000) Involvement of caspase-3 in epigallocatechin-3-gallate-mediated apoptosis of human chondrosarcoma cells. Biochem. Biophys. Res. Commun. **270**, 793–797

17 Sun, X. M., MacFarlane, M., Zhuang, J., Wolf, B. B., Green, D. R. and Cohen, G. M. (1999) Distinct caspase cascades are initiated in receptor-mediated and chemical-induced apoptosis. J. Biol. Chem. **274**, 5053–5060

18 Tobiume, K., Saitoh, M. and Ichijo, H. (2002) Activation of apoptosis signal-regulating kinase 1 by the stress-induced activating phosphorylation of pre-formed oligomer. J. Cell. Physiol. **191**, 95–104

19 Bennett, B. L., Sasaki, D. T., Murray, B. W., O'Leary, E. C., Sakata, S. T., Xu, W., Leisten, J. C., Motiwala, A., Pierce, S., Satoh, Y. et al. (2001) SP600125, an anthrapyrazolone inhibitor of Jun N-terminal kinase. Proc. Natl. Acad. Sci. U.S.A. **98**, 13681–13686

20 Ichijo, H., Nishida, E., Irie, K., ten Dijke, P., Saitoh, M., Moriguchi, T., Takagi, M., Matsumoto, K., Miyazono, K. and Gotoh, Y. (1997) Induction of apoptosis by ASK1, a mammalian MAPKKK that activates SAPK/JNK and p38 signaling pathways. Science **275**, 90–94

21 Matsuda, S., Moriguchi, T., Koyasu, S. and Nishida, E. (1998) T lymphocyte activation signals for interleukin-2 production involve activation of MKK6-p38 and MKK7-SAPK/JNK signaling pathways sensitive to cyclosporin A. J. Biol Chem. **273**, 12378–12382

22 Yasuda, S., Inoue, K., Hirabayashi, M., Higashiyama, H., Yamamoto, Y., Fukuhiro, H., Komure, O., Tanaka, F., Sobue, G., Tsuchiya, K. et al. (1999) Triggering of neuronal cell death by accumulation of activated SEK1 on nuclear polyglutamine aggregations in PML bodies. Gene Cells **4**, 743–756

23 Noguchi, K., Kitanaka, C., Yamana, H., Kakubu, A., Mochizuki, T. and Kuchino, Y. (1999) Regulation of c-Myc through phosphorylation at Ser-62 and Ser-71 by c-Jun N-terminal kinase. J. Biol. Chem. **274**, 32580–32587

24 Nara, N. (1992) Colony-stimulating factor (CSF)-dependent growth of two leukemia cell lines. Leuk. Lymphoma **7**, 331–335

25 Sellins, K. S. and Cohen, J. J. (1987) Gene induction by gamma-irradiation leads to DNA fragmentation in lymphocytes. J. Immunol. **139**, 3199–3206

26 Okuma, E., Saeki, K., Shimura, M., Ishizaka, Y., Yasugi, E. and Yuo, A. (2000) Induction of apoptosis in human hematopoietic U937 cells by granulocyte-macrophage colony-stimulating factor: possible existence of caspase 3-like pathway. Leukemia **14**, 612–619

27 Hamm, A., Krott, N., Breibach, I., Blindt, R. and Bosserhoff, A. K. (2002) Efficient transfection method for primary cells. Tissue Eng. **8**, 235–245

28 Schreiber, E., Matthias, P., Muller, M. M. and Schaffner, W. (1989) Rapid detection of octamer binding proteins with 'mini-extracts', prepared from a small number of cells. Nucleic Acids Res. **17**, 6419

29 Lee, J. C., Laydon, J. T., McDonnell, P. C., Gallagher, T. F., Kumar, S., Green, D., McNulty, D., Blumenthal, M. J., Heys, J. R., Landvatter, S. W. et al. (1994) A protein kinase involved in the regulation of inflammatory cytokine biosynthesis. Nature (London) **372**, 739–746

30 Cambien, B., Pomeranz, M., Millet, M. A., Rossi, B. and Schmid-Alliana, A. (2001) Signal transduction involved in MCP-1-mediated monocytic transendothelial migration. Blood **97**, 359–366

31 Jacinto, E., Werlen, G. and Karin, M. (1998) Cooperation between Syk and Rac1 leads to synergistic JNK activation in T lymphocytes. Immunity **8**, 31–41

32 Adrain, C. and Martin, S. J. (2001) The mitochondrial apoptosome: a killer unleashed by the cytochrome seas. Trends Biochem. Sci. **26**, 390–397

33 Henkel, T., Machleidt, T., Alkalay, I., Kronke, M., Ben-Neriah, Y. and Baeuerle, P. A. (1993) Rapid proteolysis of IκB-α is necessary for activation of transcription factor NF-κB. Nature (London) **365**, 182–185

34 Slee, E. A., Harte, M. T., Kluck, R. M., Wolf, B. B., Casiano, C. A., Newmeyer, D. D., Wang, H. G., Reed, J. C., Nicholson, D. W., Alnemri, E. S. et al. (1999) Ordering the cytochrome c-initiated caspase cascade: hierarchical activation of caspases-2, -3, -6, -7, -8, and -10 in a caspase-9-dependent manner. J. Cell Biol. **144**, 281–292
35 Davis, Jr, W., Ronai, Z. and Tew, K. D. (2001) Cellular thiols and reactive oxygen species in drug-induced apoptosis. J. Pharmacol. Exp. Ther. **296**, 1–6
36 Saitoh, M., Nishitoh, H., Fujii, M., Takeda, K., Tobiume, K., Sawada, Y., Kawabata, M., Miyazono, K. and Ichijo, H. (1998) Mammalian thioredoxin is a direct inhibitor of apoptosis signal-regulating kinase (ASK) 1. EMBO J. **17**, 2596–2606
37 Jankun, J., Selman, S. H., Swiercz, R. and Skrzypczak-Jankun, E. (1997) Why drinking green tea could prevent cancer. Nature (London) **387**, 561
38 Meister, A. and Anderson, M. E. (1983) Glutathione. Annu. Rev. Biochem. **52**, 711–760
39 Griffith, O. W. and Meister, A. (1979) Potent and specific inhibition of glutathione synthesis by buthionine sulfoximine (S-n-butyl homocysteine sulfoximine). J. Biol. Chem. **254**, 7558–7560
40 Dai, J., Weinberg, R. S., Waxman, S. and Jing, Y. (1999) Malignant cells can be sensitized to undergo growth inhibition and apoptosis by arsenic trioxide through modulation of the glutathione redox system. Blood **93**, 268–277
41 Baud, V. and Karin, M. (2001) Signal transduction by tumor necrosis factor and its relatives. Trends Cell Biol. **11**, 372–377
42 Varghese, J., Chattopadhaya, S. and Sarin, A. (2001) Inhibition of p38 kinase reveals a TNF-alpha-mediated, caspase-dependent, apoptotic death pathway in a human myelomonocyte cell line. J. Immunol. **166**, 6570–6577
43 Nagata, Y. and Todokoro, K. (1999) Requirement of activation of JNK and p38 for environmental stress-induced erythroid differentiation and apoptosis and of inhibition of ERK for apoptosis. Blood **94**, 853–863
44 Nguyen, L. T., Duncan, G. S., Mirtsos, C., Ng, M., Speiser, D. E., Shahinian, A., Marino, M. W., Mak, T. W., Ohashi, P. S. and Yeh, W. C. (1999) TRAF2 deficiency results in hyperactivity of certain TNFR1 signals and impairment of CD40-mediated responses. Immunity **11**, 379–389
45 Tobiume, K., Matsuzawa, A., Takahashi, T., Nishitoh, H., Morita, K., Takeda, K., Minowa, O., Miyazono, K., Noda, T. and Ichijo, H. (2001) ASK1 is required for sustained activations of JNK/p38 MAP kinases and apoptosis. EMBO Rep. **2**, 222–228
46 Torcia, M., De Chiara, G., Nencioni, L., Ammendola, S., Labardi, D., Lucibello, M., Rosini, P., Marlier, L. N., Bonini, P., Sbarba, P. D. et al. (2001) NGF inhibits apoptosis in memory B lymphocytes via inactivation of p38 MAPK, prevention of Bcl-2 phosphorylation and cytochrome c release. J. Biol. Chem. **276**, 39027–39036
47 Nanjo, F., Goto, K., Seto, R., Suzuki, M., Sakai, M. and Hara, Y. (1996) Scavenging effects of tea catechins and their derivatives on 1,1-diphenyl-2-picrylhydrazyl radical. Free Radicals Biol. Med. **21**, 895–902
48 Nanjo, F., Mori, M., Goto, K. and Hara, Y. (1999) Radical scavenging activity of tea catechins and their related compounds. Biosci. Biotechnol. Biochem. **63**, 1621–1623
49 Katiyar, S. K. and Elmets, C. A. (2001) Green tea polyphenolic antioxidants and skin photoprotection. Int. J. Oncol. **18**, 1307–1313
50 Katiyar, S. K., Afaq, F., Perez, A. and Mukhtar, H. (2001) Green tea polyphenol (−)-epigallocatechin-3-gallate treatment of human skin inhibits ultraviolet radiation-induced oxidative stress. Carcinogenesis **22**, 287–294
51 Katiyar, S. K., Afaq, F., Azizuddin, K. and Mukhtar, H. (2001) Inhibition of UVB-induced oxidative stress-mediated phosphorylation of mitogen-activated protein kinase signaling pathways in cultured human epidermal keratinocytes by green tea polyphenol (−)-epigallocatechin-3-gallate. Toxicol. Appl. Pharmacol. **176**, 110–117
52 Schreck, R., Rieber, P. and Baeuerle, P. A. (1991) Reactive oxygen intermediates as apparently widely used messengers in the activation of the NF-κB transcription factor and HIV-1. EMBO J. **10**, 2247–2258
53 Smith, C. A., Farrah, T. and Goodwin, R. G. (1994) The TNF receptor superfamily of cellular and viral proteins: activation, costimulation, and death. Cell **76**, 959–962
54 Piette, J., Piret, B., Bonizzi, G., Schoonbroodt, S., Merville, M. P., Legrand-Poels, S. and Bours, V. (1997) Multiple redox regulation in NF-κB transcription factor activation. Biol. Chem. **378**, 1237–1245
55 Ginn-Pease, M. E. and Whisler, R. L. (1998) Redox signals and NF-κB activation in T cells. Free Radicals Biol. Med. **25**, 346–361
56 Chandel, N. S., Schumacker, P. T. and Arch, R. H. (2001) Reactive oxygen species are downstream products of TRAF-mediated signal transduction. J. Biol. Chem. **276**, 42728–42736
57 Mouria, M., Gukovskaya, A. S., Jung, Y., Buechler, P., Hines, O. J., Reber, H. A. and Pandol, S. J. (2002) Food-derived polyphenols inhibit pancreatic cancer growth through mitochondrial cytochrome C release and apoptosis. Int. J. Cancer **98**, 761–769

Received 15 January 2002/19 August 2002; accepted 3 September 2002
Published as BJ Immediate Publication 3 September 2002, DOI 10.1042/BJ20020101